# Marine and terrestrial influences on ice nucleating particles during continuous springtime measurements in an Arctic oilfield location

Jessie M. Creamean[1,2], Rachel M. Kirpes[3], Kerri A. Pratt[3], Nicholas J. Spada[4], Maximilian Maahn[1,2], Gijs de Boer[1,2], Russell C. Schnell[5], Swarup China[6]

[1]Cooperative Institute for Research in Environmental Sciences, University of Colorado, Boulder, CO, 80309, USA
[2]Physical Sciences Division, National Oceanic and Atmospheric Administration, Boulder, CO, 80305, USA
[3]Department of Chemistry, University of Michigan, Ann Arbor, MI, 48109, USA
[4]Air Quality Research Center, University of California, Davis, CA, 95616, USA
[5]Global Monitoring Division, National Oceanic and Atmospheric Administration, Boulder, CO, 80305, USA
[6]Environmental and Molecular Sciences Laboratory, Pacific Northwest National Laboratory, Richland, WA, 99352, USA

*Correspondence to*: Jessie M. Creamean (jessie.creamean@noaa.gov)

**Abstract.** Aerosols that serve as ice nucleating particles (INPs) have the potential to modulate cloud microphysical properties and can therefore impact cloud radiative forcing and precipitation formation processes. In remote regions such as the Arctic, aerosol-cloud interactions are severely understudied yet may have significant implications for the surface energy budget and its impact on sea ice and snow surfaces. Further, uncertainties in model representations of heterogeneous ice nucleation are a significant hindrance to simulating Arctic mixed-phase cloud processes. We present results from a campaign called INPOP (Ice Nucleating Particles at Oliktok Point), which took place at a U.S. Department of Energy Atmospheric Radiation Measurement (DOE ARM) facility in the northern Alaskan Arctic. Three time- and size-resolved aerosol impactors were deployed from 1 Mar to 31 May 2017 for offline ice nucleation and chemical analyses and were co-located with routine measurements of aerosol number, size, chemistry, and radiative properties. The largest particles (i.e., $\geq 3$ μm or "coarse mode") were the most efficient INPs. During periods with snow- and ice-covered surfaces, coarse mode INP concentrations were very low (maximum of $6 \times 10^{-4}$ L$^{-1}$ at –15 °C), but higher concentrations of warm temperature INPs were observed during late May (maximum of $2 \times 10^{-2}$ L$^{-1}$ at –15 °C). These higher concentrations were attributed to air masses originating from over sea ice leads and tundra surfaces. To our knowledge, these results represent the first INP characterization measurements in an Arctic oilfield location, and demonstrate strong influences from natural sources despite the relatively high pollution levels in this Arctic environment. Ultimately, these results can be used to evaluate the anthropogenic and natural influences on aerosol composition and Arctic cloud properties.

## 1 Introduction

Aerosols are an important component of the atmospheric system through their various impacts on climate. Depending on the type (Satheesh and Moorthy, 2005), aerosols directly scatter and/or absorb radiation, thereby affecting the atmospheric energy budget (Boucher et al., 2013). Notably, the largest uncertainty of the energy budget (i.e., radiative forcing estimate) is the

aerosol indirect effect. As cloud condensation nuclei (CCN) and ice nucleating particles (INPs), aerosols influence atmospheric radiation through modulation of the microphysics of cloud droplets and ice crystals. Aerosol-induced microphysical modifications influence cloud lifetime and albedo, as well as the production of more or less precipitation (Albrecht, 1989; Twomey, 1977). However, constraining aerosol-cloud impacts in climate models, specifically when parameterizing INPs in mixed phase cloud (MPC) systems, remains a significant challenge due to limited observations (Coluzza et al., 2017; Cziczo et al., 2017; DeMott et al., 2010; Kanji et al., 2017; Korolev et al., 2017).

The efficacy of an aerosol to serve as an INP largely depends on its composition (i.e., chemical, mineral, or biological makeup), morphology, and size, and thus, its source. INPs nucleate ice through pathways dependent upon temperature, saturation with respect to ice, and the INP size and composition (Hoose and Möhler, 2012). Immersion freezing is the most relevant to MPC formation and requires that INPs initially serve as CCN. Aerosols such as mineral dust, soil dust, sea salt, volcanic ash, black carbon from wildfires, and primary biological aerosol particles (PBAPs) have been shown to serve as INPs (Coluzza et al., 2017; Conen et al., 2011; DeMott et al., 1999; Hoose and Möhler, 2012; McCluskey et al., 2014; Murray et al., 2012; Petters et al., 2009). Among these, dust and PBAPs are the most adroit INPs found in the atmosphere (Coluzza et al., 2017; Murray et al., 2012). PBAPs originating from certain bacteria and vegetative detritus are the most efficient INPs known, capable of initiating freezing near −1°C, while most PBAPs (e.g., pollen, fungal spores, algae, and diatoms) tend to nucleate ice at temperatures similar to those of mineral dust but warmer than sea salt or volcanic ash (Alpert et al., 2011; Creamean et al., 2014; Creamean et al., 2013; Despres et al., 2012; Durant et al., 2008; Fröhlich-Nowoisky et al., 2015; Hader et al., 2014b; Hill et al., 2016; Hoose and Möhler, 2012; Knopf et al., 2010; McCluskey et al., 2014; Murray et al., 2012; O'Sullivan et al., 2014; Tesson et al., 2016; Tobo et al., 2014; Umo et al., 2015). However, dusts can serve as atmospheric shuttles for small microbes, enabling these particle mixtures to behave more efficiently as INPs compared to the dust alone (Conen et al., 2011; Creamean et al., 2013; O'Sullivan et al., 2014). Consequently, PBAPs have the potential to play a crucial role in cloud ice formation (Creamean et al., 2014; Creamean et al., 2013; Pratt et al., 2009) and precipitation enhancement (Bergeron, 1935; Christner et al., 2008; Morris et al., 2014; Morris et al., 2004; Morris et al., 2017; Stopelli et al., 2014), particularly in the presence of supercooled water or large cloud droplets. PBAPs have been a key focus of recent ice nucleation studies, yet estimating their global impact remains a challenge due to: 1) a dearth of observations in time and space and 2) a poor understanding of sources, flux, and abundance of PBAPs in the Earth-atmosphere system (Hoose et al., 2010a).

Little is known about marine emissions of biological INPs—most studies of such aerosols to date have examined terrestrial sources (Burrows et al., 2013; Murray et al., 2012). Recent laboratory, field, and modelling studies have evaluated the mechanical emission processes, ice nucleation efficiency, and concentrations of INPs generated from marine environments (DeMott et al., 2016; Knopf et al., 2010; McCluskey et al., 2017). Results from these studies imply that PBAPs are most relevant to ice formation at MPC temperatures (i.e., > −10°C), whereas sea salt aerosols nucleate ice in both deposition and immersion modes at temperatures relevant for cirrus clouds (i.e., < −38°C) (Schill and Tolbert, 2014). Conclusions on the role

of PBAPs in ice nucleation and precipitation are equivocally based on results from climate modelling, with some studies implying they are insignificant on a global scale (Hoose et al., 2010a; Hoose et al., 2010b; Sesartic et al., 2012), while others have found them to be potentially important (Phillips et al., 2009; Phillips et al., 2008; Vergara-Temprado et al., 2017). An inherent limitation of these pioneering studies is that results were validated by a handful of terrestrial-based observations of

5 biological INPs. This, coupled with the fact that the Earth's surface is 70% covered by ocean, implies that studies using global climate simulations have ignored a potentially significant global source of INPs.

Previous work by Leck and Bigg in the High Arctic were among the first to elucidate the potentially paramount role of the ocean as a microbial source of efficient INPs (Bigg, 1996; Bigg and Leck, 2001, 2008; Leck and Bigg, 2005). However, new studies that provide information on key sources of INPs *and* their impacts on Arctic MPCs are necessary to assess the direct

10 contribution from the marine environment. Irish et al. (2017) and Wilson et al. (2015) report enhanced ice nucleation activity of particulate matter in the surface microlayer and bulk seawater from the Arctic Ocean. In addition, sources of INPs at coastal locations have been measured during the summer by Fountain and Ohtake (1985), Mason et al. (2016), and Conen et al. (2016) in Alaska, Canada, and Norway, respectively, but were likely impacted, if not mostly dominated by, terrestrial sources. To date, only a handful of studies have evaluated Arctic INPs in coastal or marine environments.

15 The Arctic is a remarkable region with regard to many atmospheric processes, but especially with regard to ice nucleation because: 1) the Arctic is mostly ocean, which may be the most prolific regional source of biological INPs, 2) interruption of ocean-atmospheric exchange by sea ice cover likely affects seasonally-dependent patterns in the emission of PBAPs/INPs, and 3) aerosol-cloud interactions could have implications important to understanding declining trends in sea ice and snow coverage. Overall, limited information on aerosol-cloud processes (Garrett and Zhao, 2006; Lubin and Vogelmann, 2006), contradictory

20 modelling results with regard to the importance of biological INPs (Szyrmer and Zawadzki, 1997), and a critical need to understand the role of aerosol particles in determining cloud phase (Bergeron, 1935; Findeisen, 1938; Wegener, 1911) motivate the need for additional observations to constrain the abundance and ice-nucleating properties of aerosols in the Arctic (Murray et al., 2012). Here, we present a 3-month record of continuous time- and size-resolved INP concentrations at Oliktok Point, a coastal site in Northern Alaska situated within the North Slope of Alaska (Prudhoe Bay) oilfields, which have been shown to

25 be strong and localized sources of pollutants in this region (Creamean et al., 2018a; Maahn et al., 2017). Unique observations of an increase in what were likely marine- and terrestrial-sourced INPs are discussed. This is the first time INP measurements have been conducted in an Arctic oilfield, and we demonstrate how efficient, natural INPs are likely important in such a relatively polluted Arctic location.

## 2 Methods

### 2.1 Study location and dates

INPOP was conducted at the Third Atmospheric Radiation Measurement (ARM) Mobile Facility (AMF-3) operated by the United States Department of Energy (DOE) in Oliktok Point, Alaska (70.51°N, 149.86°W, 2 meters above mean sea level (m

5  a.m.s.l.)) (Creamean, 2017b). Oliktok Point is located in Prudhoe Bay (Figure 1), the third largest oilfield in North America (U.S. Energy Information Administration, 2015). The study time period was 1 Mar – 31 May 2017. Data from INPOP and the rest of the AMF-3 data record (2013 – present) are available on the ARM data archive (https://www.archive.arm.gov/discovery/) (Creamean, 2017a).

### 1.2 Sample collection

10  For offline ice nucleation analyses, daily aerosol samples were collected 11 Mar – 31 May 2017 (Table 1) using a 4-stage time- and size-resolved Davis Rotating-drum Universal-size-cut Monitoring (DRUM) single-jet impactor (DA400, DRUMAir, LLC.) (Cahill et al., 1987) housed in a 47 x 35.7 x 17.6 cm Pelican™ case (inset in Figure 1). The DRUM collected aerosol particles at four size ranges (0.15 – 0.34, 0.34 – 1.20, 1.20 – 2.96, and 2.96 – >12 µm in Stokes' equivalent diameter) and sampled at 26.7 L min$^{-1}$, equalling 38428 total L of air per day (i.e., per sample). Such size ranges cover a wide array of

15  aerosols, particularly those that serve as INPs (DeMott et al., 2010; Fridlind et al., 2012; Mason et al., 2016). Simultaneously, the large volume of air collected promotes collection of rarer warm temperature biological INPs, which may represent a lower fraction of overall INP concentrations (Mossop and Thorndike, 1966). Samples were deposited onto 20 x 190 mm strips of petrolatum-coated (100%, Vaseline®) Mylar™ (0.02 mm thick; DuPont®) substrate secured onto the rotating drums (20 mm thick, 60 mm in diameter) in each of the four stages at the rate of 7 mm per day (5 mm of sample streaked onto the Mylar

20  followed by 2 mm of blank).

The DRUM was secured inside the AMF-3 container, with an approximately 7-m long sampling line (6.4 mm inner diameter static-dissipative polyurethane tubing; McMaster-Carr®) leading to outside of the container and connected to a plastic funnel inlet covered with loose mosquito netting to prevent rimed ice build-up or blowing snow from clogging the inlet. Daily rotation checks were conducted by disconnecting the DRUM from its pump and removing the stage caps to ensure the drums were

25  rotating at the correct rate and sample substrates remained secured to each drum. Weekly checks of the inlet flow and pressure measured at each stage were conducted to ensure the orifices to each stage were not clogged and the DRUM pump was operating correctly.

The drums rotated for 24 to 26 days before sample substrates were changed (i.e., one full rotation of the drums), equalling three drum changes during INPOP. Sampled substrates were kept on the drums and stored frozen in a standard freezer until

30  transport to Boulder, Colorado and stored frozen in a chest freezer for 5 to 7 months before offline INP analyses (see following

section). This is the first time a DRUM has been used for offline INP analyses, but as we demonstrate, it is a useful sample collection method for long-term studies.

For offline single-particle analysis, daily samples were collected at 16.1 L min$^{-1}$ using a 3-stage DRUM impactor with particle size ranges 0.10 – 0.34 µm, 0.34 – 1.15 µm, and >1.15 µm on transmission electron microscopy (TEM) grids (Formvar carbon Type-B copper grids, Ted Pella, Inc.) attached to each of the three drums. The rotation was set at 3 mm per day, such that particles were deposited over the width of one TEM grid per 24-hour sampling period. Drums were changed once over the course of the INPOP study. Sampled substrates were kept on the drums and stored in the dark at ambient temperature until analysis (~3 months) (Laskina et al., 2015). Select daily samples corresponding to interesting case studies were analysed for discussion in the current paper. A third DRUM sampler collecting particles in 8 size bins (0.09 – 0.26 µm, 0.26 – 0.34 µm, 0.34 – 0.56 µm, 0.56 – 0.75 µm, 0.75 – 1.15 µm, 1.15 – 2.5 µm, 2.5 – 5.0 µm, and 5.0 – >12 µm) on Mylar™ for 12 hours per sample was co-located for bulk inorganic analysis (~2 months after collection). The flow rate was maintained at 9.6 L min$^{-1}$ with a drum rotation rate of 0.5 mm per day. Only one set of drums for this sampler was needed for the duration of INPOP. Samples were stored in the DRUM chambers during shipment and storage until analysis. The same sampling line set ups and routine checks as for the 4-stage DRUM were applied to the 3-stage and 8-stage DRUMs.

## 1.2 Drop freezing assays (DFA) for immersion mode INPs

In total, 216 daily samples were collected between the four different stages (herein, stages A, B, C, and D correspond to 2.96 – 12, 1.20 – 2.96, 0.34 – 1.20, and 0.15 – 0.34 µm particles, respectively. Due to contamination issues, stages B and D were not analysed from the first set of daily samples (see Table 1). Other missing data (i.e., samples not analysed) are due to occasional power outages at the AMF-3. Due to the large volume of samples, initially, one daily sample per week was analysed to assess a broader picture of INPs over the course of the spring months. Daily samples were analysed 22 – 29 May 2017 due to interesting aerosol events observed during this time period. Immediately prior to analysis, sample strips were cut into their daily segments and stored frozen in 29-mL sterile Whirlpak® bags for up to one week.

Immersion mode freezing was tested using a DFA cold plate apparatus. This cold plate technique was based on previous but slightly modified apparatuses (Hill et al., 2016; Stopelli et al., 2014; Tobo, 2016; Wright and Petters, 2013) and discussed in detail by Creamean et al. (2018b). For brevity, we call this system the Drop Freezing Cold Plate (DFCP). Before analysing with the DFCP, 2 mL of ultrapure water (UPW; Barnstead™ Smart2Pure™ 6 UV/UF) were added to the sterile Whirlpak® bags containing sample segments to resuspend deposited particles. The bags were sealed and shaken at 500 rpm for two hours (Bowers et al., 2009). Copper discs (76 mm in diameter, 3.2 mm thick) were prepared by cleaning with isopropanol (99.5% ACS Grade, LabChem. Inc.), then coating with a thin layer of petrolatum (Bowers et al., 2009; Tobo, 2016). Following sample preparation, a sterile, single-use plastic syringe was used to draw 0.25 mL of the suspension and 100 drops were pipetted onto the petrolatum-coated copper disc, creating an array of ~2.5-µL aliquots. Drops were visually inspected for size; however, it

is possible not all drops were the same exact volume, which could lead to a small level of indeterminable uncertainty (Alpert and Knopf, 2016). However, we have previously demonstrated that drop size variability does not impact freezing results (Creamean et al., 2018b). Previous studies have elucidated that drops need to be orders of magnitude different in volume to significantly perturb the freezing temperature from drop size, alone (Bigg, 1953; Hader et al., 2014a; Langham and Mason, 1958). The copper disc was then placed on a thermoelectric cold plate (Aldrich®) and covered with a transparent plastic dome. Small holes in the side of the dome and copper disc permitted placement of up to four temperature probes using an Omega™ thermometer/data logger (RDXL4SD; 0.1 °C resolution and accuracy of $\pm$ (0.4% + 1 °C) for the K sensor types used). During the test, the cold plate was cooled variably within a 1 – 10 °C min$^{-1}$ range from room temperature until around −30 °C. Control experiments with UPW at various cooling rates within this range show no discernible dependency of drop freezing on cooling rate (Creamean et al., 2018b), akin to previous works (Vali and Stansbury, 1966; Wright and Petters, 2013).

A +0.33 °C correction factor was added to any temperature herein and an uncertainty of 0.15 °C was added to the probe accuracy uncertainty based on DFCP characterization testing presented in Creamean et al. (2018b), to account for the temperature difference between the measurement (i.e., in the plate centre) and actual drop temperature. Frozen drops were detected visually, but the freezing temperature and cooling rate of each drop frozen was recorded through custom software. The test continued until all 100 drops were frozen or when the system reached approximately −30 °C. Each sample was tested three times with 100 new drops for each test. From each test, the fraction frozen and percentage of detected frozen drops were calculated. For INPOP, 71 – 100% of the 100 drops were visually detected and recorded as frozen for each test. The results from the triplicate tests were then binned every 0.5 °C to produce one spectrum per sample. Cumulative INP spectra were calculated using the equation posed by Vali (1971) and adjusted to account for the total volume of air per sample:

$$[INPs(T)](L^{-1}) = \frac{\ln N_o - \ln N_u(T)}{V_{drop}} \times \frac{V_{suspension}}{V_{air}}$$

where $N_o$ is the total number of drops, $N_u(T)$ is the number of unfrozen drops at each temperature, $V_{drop}$ is the average volume of each drop, $V_{suspension}$ is the volume of the suspension (i.e., 0.75 mL total for the three tests), and $V_{air}$ is the volume of air per sample (38428 L) (Boose et al., 2016a; Chen et al., 2018; Mason et al., 2016; Stopelli et al., 2014).

**1.3 Single-particle and bulk aerosol composition**

Particles collected on TEM grids using the 3-stage DRUM were analysed for single-particle chemical composition and morphology using computer-controlled scanning electron microscopy with energy dispersive X-ray spectroscopy (CCSEM-EDX). Samples were analysed using a FEI Quanta scanning electron microscope with a field emission gun operating at 20 keV and equipped with a high angle annular dark field detector for particle size and morphology, and an energy dispersive X-ray X-ray spectrometer (EDAX, Inc.) and a Si(Li) detector (10 mm$^2$) for particle elemental composition of elements including C, N, O, Na, Mg, Al, Si, P, S, Cl, K, Ca, Ti, V, Fe, Ni, and Zn. An average of 1000 particles were analysed per substrate. Data

was analysed using k-means cluster analysis of the single-particle EDX spectra (Ault et al., 2012). Fifty clusters were combined into six classes of particle types, including fresh sea spray aerosol, aged sea spray aerosol, dust, organic aerosol, fly ash, and soot, based on similarity of elemental composition (Gunsch et al., 2017; Kirpes et al., 2018; Weinbruch et al., 2012).

Samples collected on the 8-stage DRUM were analysed for elemental concentrations using synchrotron-induced X-ray fluorescence spectrometry (S-XRF) at the Lawrence Berkeley National Laboratory Advanced Light Source facility (Perry et al., 2004; VanCuren et al., 2012). The 1.5 GeV polarized X-ray beam provides very low background bremsstrahlung radiation and high sensitivity of elements including Na, Mg, Al, Si, P, S, Cl, Ar, K, Ca, Sc, Ti, V, Cr, Mn, Fe, Co, Ni, Cu, Zn, Ga, Ge, As, Se, Br, Rb, Sr, Y, Zr, Nb, Mo, and Pb. Spectra were acquired with a Vortex-60EX silicon drift detector (Hitachi High Technologies, USA) and were post-processed using both WinAXIL (Canberra, Belgium) and PyMca (Sole et al., 2007) independently, for quality assurance. Further data reduction into timestamped concentrations was performed using custom software (R Foundation for Statistical Computing, 2017). For specific comparisons, non-soil K was calculated as *non-soil-K = K − 0.45 × Fe* (Lewis et al., 1988) while soil K was calculated as *soil-K = K – non-soil-K*. These estimations ignore any contribution from biomass burning, which was a minor component of the observed single-particle designations.

## 1.4 Supporting observations and modelling

The AMF-3 at Oliktok Point includes the ARM Aerosol Observing System (AOS), which provides a wide range of aerosol and meteorological measurements (Jefferson, 2011). Data used here are publicly available in the ARM data archive and include aerosol number and size and wind direction and speed. Aerosol number concentrations were measured with a condensation particle counter (CPCf; 10 nm – 3 µm) and ultrafine CPC (CPCu; 3 nm – 3 µm) (TSI, Inc. models 3010 and 3025, respectively). Aerosol size distributions were measured with an ultrahigh-sensitivity aerosol sizer (UHSAS, Droplet Measurement Technologies, Inc.) for particles in the 60 nm – 1 µm size range. The AOS Surface Meteorology (AOSMET) data for atmospheric temperature, humidity, and wind speed and direction were measured via a Vaisala, Inc. WXT520 Weather Transmitter (Kyrouac, 2016). AOS data have a time resolution of 1 second.

Daily snow and ice cover data were obtained from the National Snow & Ice Data Center. Snow cover data (http://nsidc.org/data/g02156#table3, Version 1) were derived from the Ice Mapping System (IMS) daily northern hemisphere snow analysis at a 1 km x 1 km resolution and are derived from a variety of data products including satellite imagery and in situ data (National Ice Center, 2008). Sea ice data (https://nsidc.org/data/g10005, Version 1) were derived from the Multisensor Analyzed Sea Ice Extent Advanced Microwave Scanning Radiometer 2 MASIE-AMSR2 (MASAM2) daily 4 km sea ice concentration product that is a blend of two other daily sea ice data products: ice coverage from the product at a 4 km grid cell size and ice concentration from the AMSR2 at a 10 km grid cell size (Fetterer et al., 2015). MASAM2 was used to meet a need for greater accuracy and higher resolution in ice concentration fields. Air mass backward trajectories (5-day) were calculated using the HYbrid Single Particle Lagrangian Integrated Trajectory model with the SplitR package for RStudio

(https://github.com/rich-iannone/SplitR) (Draxler, 1999; Draxler and Rolph, 2011). Data from the Global Data Assimilation System (GDAS; 1˚ latitude-longitude; 3-hourly) from National Centers for Environmental Prediction (NCEP) were used as the meteorological fields in HYSPLIT simulations. Trajectories were initiated at 5 m above ground level (a.g.l.) (i.e., approximate height of the inlet) every 3 hours daily. Only hours within the sample day (i.e., starting at 16:00 UTC) were

5    evaluated per each sample such that 18:00 and 21:00 on the same day and 00:00, 03:00, 06:00 09:00, 12:00, and 15:00 on the following day were considered per sample. Trajectories were only simulated for each day of May during sea ice melt off the Alaskan coast and during the 22 – 29 May case study.

## 3 Results and discussion

### 3.1 Atmospheric conditions during INPOP

10   Shifts in the aerosol population and atmospheric conditions throughout the course of INPOP were evident from the AOS measurements (Figure 2). Particle concentrations were in general relatively high, with the CPCu, CPCf and UHSAS measuring average concentrations of 2065, 1589, and 1479 cm$^{-3}$, respectively, over the entire study. These elevated concentrations are likely the result of the local industrial activities, which are prominent at Oliktok Point (Creamean et al., 2018a; Gunsch et al., 2017; Maahn et al., 2017). Akin to previous work on the North Slope during the Arctic haze, high particle concentrations were

15   observed in April (e.g., Quinn et al., 2007), with averages of 2056, 3329, and 1532 cm$^{-3}$ for CPCu and 1677, 2769, and 896 cm$^{-3}$ for CPCf measured from March, April, and May, respectively. The monthly averaged UHSAS concentration was highest in March, at concentrations much higher than measured in May (3050, 1652, and 975 cm$^{-3}$ for March, April, and May, respectively). However, data from March may not be representative of the entire month due to a power outage in the first part of that month (i.e., missing data in Figure 2). As documented in previous studies (Di Pierro et al., 2013; Garrett et al., 2010;

20   Law and Stohl, 2007; Stohl, 2006), changes in transport and precipitation patterns resulted in relatively 'cleaner' conditions, including lower particle concentrations around late May. Ambient temperature and relative humidity increased steadily over the course of the study and reached values indicative of coastal marine conditions towards the end of May (Cox et al., 2012). March winds frequently originated from the south/southwest, while winds were predominantly northerly/north-easterly during April and May. As demonstrated in the current paper, an observed shift in atmospheric conditions at Oliktok Point influenced

25   the aerosol and additionally the INP population.

### 3.2 Observation of a shift in springtime INP glaciation temperatures and concentrations in Prudhoe Bay

INP concentrations from the Arctic are typically very low compared to other regions (Kanji et al., 2017), and industrial regions are not thought to serve as prolific INP sources (e.g., Chen et al., 2018). Figure 3 shows the size-resolved INP concentrations from INPOP. A few key features are evident: (1) larger particles were more efficient INPs, especially at warmer temperatures,

30   (2) larger particles exhibited a larger spread in INP spectra, and (3) late May samples contained particularly high concentrations of warm temperature (i.e., > −10 °C) INPs relative to March and April. INPOP INP concentrations were generally low, falling

into the lower end of ranges reported by Kanji et al. (2017) and Petters and Wright (2015). Comparison of our results to previous ice nucleation studies in the Arctic are discussed in section 4.

The first feature discussed above has been reported by other size-resolved Arctic INP studies. Mason et al. (2016) report similar observations in Alert, Canada, where 95% and 70% of INPs were found at sizes > 1 μm and > 2.5 μm in diameter, respectively,

5    and a median diameter of approximately 3 μm for all INPs at –15 ˚C. In general, observational studies in locations outside of the Arctic also report a relationship between temperature and particle size, where supermicron or coarse mode aerosols are the most proficient INPs at warmer temperatures (Conen et al., 2017; Huffman et al., 2013; references cited in Mason et al., 2016; Vali, 1966). However, modelling studies suggest INPs can be as small as 500 nm (DeMott et al., 2010; DeMott et al., 2015; Fridlind et al., 2012), while observational work suggests that nanometre-sized INPs are typically found attached to larger

10   particles in the atmosphere (O'Sullivan et al., 2015). The second feature (larger spread in INP concentrations between samples with increasing size) indicates a larger variation in different aerosol sources (Seinfeld and Pandis, 2016) versus the smallest INPs observed which have similar spectra, indicating similar sources. Additionally, stage A of the DRUM has a wider size range (~9 μm) versus the smaller stages (~0.2 to 2 μm). The third reported feature was unexpected, given the characteristically polluted atmosphere in the Prudhoe Bay area. The 22 – 29 May period featured INP concentrations up to $4 \times 10^{-3}$ L$^{-1}$ at −10

15   °C and $2 \times 10^{-2}$ L$^{-1}$ at −15 °C, with warm temperature INPs apparent especially for the largest sizes (i.e., 2.96 – > 12 μm (stage A) and 1.21 – 2.96 μm (stage B)). The onset temperatures (up to −5 °C) were also much higher during this period for the two largest size cuts of the DRUM (Figure 4), indicating a presence of biological INPs (Kanji et al., 2017; Murray et al., 2012). The presence of biological INPs in Prudhoe Bay in the spring are somewhat unexpected given the predominantly frozen surfaces. Despite this, the sizes of the observed INPs indicates a more local or regional origin due to reduced atmospheric

20   lifetime (Jaenicke, 1980). The smallest sizes (0.34 – 1.21 μm (stage C) and 0.15 – 0.34 μm (stage D)) did not portray the same trend during late May. There, a higher fraction of particles was active at much colder temperatures (i.e., INP$_{-20}$ and INP$_{-25}$) as compared to INP$_{-10}$ or INP$_{-15}$, where temperatures are generally relevant to less efficient biological INPs (i.e., spores) and mineral dust (Boose et al., 2016b; Haga et al., 2014; Murray et al., 2012). A previous study by Stone et al. (2007) demonstrated transport of Asian dust to Utqiaġvik during the spring, thus, introducing sources of colder temperature INPs even though the

25   surface is predominantly frozen.

### 3.3 Open Arctic leads and snow melt over tundra as sources of observed transition in INP properties

Focusing on the month of May, it is clear that there are higher concentrations of warm temperature INPs, particularly for DRUM stages A and B (Figure 4). Stages C and D include, or are completely composed of, particles that are theoretically thought to be too small to serve as efficient INPs (DeMott et al., 2010; DeMott et al., 2015; Fridlind et al., 2012), which is

30   consistent with the low INP activity from such particles during INPOP. Stage A was especially unique, with the range of freezing temperatures becoming smaller over time. To investigate this range in more detail, we define a parameter, ΔT, which is calculated by subtracting the first onset freezing temperature from the lowest freezing temperature detected (Figure 5). There

were no notable trends with ΔT from the other stages. Although ΔT was larger on 16 May for stage A, the highest onset freezing temperature from the entire study was observed during this day as indicated in the previous section. Snow coverage decreased sharply within 700 km of Oliktok Point on 8 May, while sea ice within 700 km dropped in fraction after 13 May (Figure 5e), which roughly aligns with the increase in onset freezing temperature and lower ΔT values for the largest particles

5    in stage A and generally higher onset freezing temperatures for stages B and C.

The observed increase of warm temperature INPs at Oliktok Point can be attributed to air mass transport pathways and timescales. Transport of regional air was quite slow and remained predominantly near the surface, as evidenced by the 5-day air mass back trajectories shown in Figure 6. At the beginning of May, frozen surfaces were prominent across the entire region, including the areas over which air transported to Oliktok Point travelled. Starting 16 May, several leads and polynyas were

10   observed in the Beaufort Sea northeast of Oliktok Point, about 700 km away. Air mass trajectories show low-altitude transport over this region, corresponding to a slight increase in warm temperature INPs on that day and the warmest onset temperatures (Figure 5a). However, due to the distance between Oliktok and the open water, particles within the size range of stage A likely gravitationally settled during the 5-day transit. On 22 May, there was a significant shift in air mass origin: air reaching Oliktok Point originated from over a large area of open leads within 30 km off the coast of Utqiaġvik (Figure 6d). This shift

15   corresponded to the highest INP concentrations and lowest ΔT observed from any sample analysed. Sources were generally regional in nature, with locations directly north of Oliktok Point until 26 May, after which they transitioned to originating predominantly south of Oliktok Point, from exposed tundra over the terrestrial North Slope. ΔT decreased slightly from 26 May onward, but INP concentrations remained high relative to earlier on during INPOP. Onset temperatures decreased following 26 May and INP concentrations remained high, but for colder freezing temperatures (i.e., –25 ˚C; Figure 4a). On 29

20   May, ΔT and INP concentrations dropped and air masses transitioned to originating from predominantly over frozen surfaces.

Colocated single-particle and bulk chemistry measurements support the sources of the air masses during the transition period in late May (Figure 7). Here, we briefly discuss results from the compositional analyses in support of the ice nucleation measurements. Analysis of May periods by CCSEM-EDX identified marine, terrestrial, and combustion influences based on particle composition and air mass trajectories (Figure 7a – d). Particle types from marine (fresh and aged sea spray aerosol

25   (SSA)) and terrestrial (dust) sources comprised the greatest number fractions of supermicron (> 1.15 µm) aerosol particles for all samples (54 % and 37 %, respectively). Each May sample demonstrated a large fraction of marine influence, with nearly 50% of supermicron particles, by number, comprised of fresh and aged SSA. The largest marine influence was observed on 23 May when air masses originated from the north over open water, local wind speeds were low and northerly, and INP concentrations, particularly in the warm temperature regime, were elevated compared to samples prior to 22 May. However,

30   periods with more terrestrial influence were observed, based on increased number fractions of supermicron dust and southerly winds on 24 May (Figure 7e). Additionally, some periods experienced more combustion influence, from local industrial emissions, characterized by relatively greater fractions of organic aerosol, fly ash, and soot (Gunsch et al., 2017; Kirpes et al.,

2018) observed by CCSEM-EDX on 28 May. The S-XRF data (0.75 – 5.0 µm) also demonstrated influences from marine and terrestrial sources, but had the highest marine signature (i.e., from fresh sea salt indicated by the Cl mass concentrations) 16 – 20 May when local winds were elevated (~ 10 m s$^{-1}$) and originated from the north over the Beaufort Sea. The S-XRF indicated the highest dust influence was observed from 25 – 30 May when episodic southerly winds from over the tundra influenced Oliktok Point (Figure 7e).

## 4 Comparison to other Arctic INP measurements

Immersion mode INP measurements in the Arctic are rare, but here we provide a synopsis of previous measurements in comparison to ours. Table 2 shows ground-based, shipborne, and airborne studies dating back to 1976 in locations throughout the Arctic during various seasons. We excluded a review of diffusional chamber INP measurements as these instruments predominantly measure deposition mode INPs and are thus not directly comparable to our results (Cziczo et al., 2017; Kanji et al., 2017). While the objective of this comparison is to determine whether our measurements align with previous immersion mode INP observations, a detailed review of Arctic INPs is outside the scope of this manuscript.

Overall, our concentrations at selected temperatures were within range of with those previously reported (Bigg, 1996; Borys, 1989; Conen et al., 2016; DeMott et al., 2016; Fountain and Ohtake, 1985; Mason et al., 2016; Radke et al., 1976), even though there are: (1) likely dependencies on time of year and location and (2) a spread by several orders of magnitude is apparent. Figure 8 shows the range of our results in comparison with those in Table 2. In general, our INP concentrations agree with or are on the lower end of those previously reported in the spring. One explanation could be that due to the proximity to the Prudhoe Bay oilfield, we are sampling in a location that is more polluted at the ground than those previously used to document Arctic haze (Borys, 1989; Mason et al., 2016; Radke et al., 1976). Additionally, Borys (1989) and Radke et al. (1976) measured via airborne platforms, in which they predominantly measured long-range transported Arctic Haze as compared to Arctic boundary layer aerosol. Other sources of variation in the results could be the result of discrepancies in the sample volumes and drop sizes used under different DFA techniques (Mossop and Thorndike, 1966; Vali, 1971). Also, unlike some of the studies presented in Table 2 and Figure 8, we collected substantial volumes of air per sample to enable measurement of the rare warm temperature INPs (38428 L in the present study versus 250 – 32400 L). Despite these differences, our concentrations are consistent with Bigg (1996), Conen et al. (2016), and DeMott et al. (2016), with those studies conducted during summer or fall. Those previous studies were apportioned to either marine or terrestrial sources, resulting in an analogous set of studies to our current effort. Overall, our measured INP concentrations are comparable to those previously conducted in a similar fashion in the Arctic and predominantly fall within the overall global picture of INPs presented by Kanji et al. and (2017) and Petters and Wright (2015).

## 5 Summary and broader implications

We present the first INP measurements in an Arctic oilfield location and demonstrate how local and regional transport from marine and terrestrial sources to an industrial region can introduce high concentrations of coarse, warm temperature INPs that are possibly of biological origin. Three time- and size-resolved aerosol impactors were deployed from 1 Mar to 31 May 2017

5 for offline ice nucleation and chemical analyses and were co-located with routine measurements of aerosol number, size, chemistry, and radiative properties. The largest particles (i.e., $\geq 3$ μm or "coarse mode") were the most efficient INPs. During periods with snow- and ice-covered surfaces, coarse mode INP concentrations were very low (maximum of $6 \times 10^{-4}$ L$^{-1}$ at –15 ˚C), but higher concentrations of warm temperature INPs were observed during late May (maximum of $2 \times 10^{-2}$ L$^{-1}$ at –15 ˚C). These higher concentrations are attributed to air masses originating from over sea ice leads and tundra surfaces. In general,

10 our concentrations agree with similar immersion mode ice nucleation evaluations at other Arctic locations, even though such studies vary in terms of location, volume of air per sample, drop freezing technique, and time of year.

Although our measurements were conducted at the ground level, such particles could influence Arctic MPC (AMPC) formation under conditions where the cloud is coupled to the surface by a well-mixed boundary layer. Previous long-term studies have evaluated the annual cycle of AMPC properties and, relevant for our measurements, have concluded that climatologically a

15 large number of AMPC occur over the North Slope of Alaska in May (up to 84 – 90% cloud fraction), with cloud bases over the North Slope reaching down below 500 – 700 m (Dong et al., 2010; Shupe, 2011; Shupe et al., 2010). Specifically, AMPC fraction is at a maximum in the fall, followed by the spring, with the lowest cloud bases occurring over the Arctic Ocean (Shupe, 2011; Shupe et al., 2006; Shupe et al., 2005). Combined, these studies indicate that INPs from surface sources may be important for such low, persistent clouds. Further, average cloud temperatures in the Arctic have been shown to be relatively

20 warm in the spring and into the summer (up to –10 ˚C on average) (de Boer et al., 2009; Shupe, 2011), indicating that biological INPs from Arctic sources are relevant to AMPC conditions typical for this time of year.

We have demonstrated that the spring to summer transition on the North Slope and beyond can have implications for a shift in INP properties, potentially impacting cloud phase, precipitation amounts, and cloud lifetime. Given significant shifts in broadband radiation regimes starting March manifesting in a sign change in cloud radiative forcing (CRF) from winter and

25 spring months to summer (Dong et al., 2010), understanding aerosol-cloud interactions is crucial during this time of year. Additionally, with increasing likelihood of earlier melting of frozen surfaces in the Arctic in coming decades (Markus et al., 2009; Screen and Simmonds, 2010; Stroeve et al., 2014), the influence of INP on CRF may be shifting in season along with the sign of CRF, with the latter resulting from a complex mix of shifting atmospheric temperature and surface albedos. Understanding the role of INPs in modulating CRF is important as this forcing can act as a positive or negative feedback on

30 the acceleration of surface melt, and the timing of such melt can potentially lead to impacts on a variety of features, midlatitude weather and climate (Cohen et al., 2018). Together, these items demonstrate a strong need to continue to improve

understanding of high latitude INPs, with additional measurements required to confirm the findings presented here, and evaluate this cycle beyond spring months.

**Acknowledgements**

We acknowledge Fred Helsel, Bruce Edwardson, and Mark Ivey for assistance in study planning, logistics, and setup. Additionally, we thank AMF-3 operators David Oaks, Ben Bishop, Joshua Remitz, and Wessley King for ensuring successful operation of the DRUM during INPOP. We also thank the members of the Oliktok Point Site Science team for their valuable feedback during data analysis, and acknowledge the NOAA Air Resources Laboratory (www.arl.noaa.gov/ready.php) and Rich Iaonnone for the provision of the SplitR HYSPLIT transport model (https://github.com/rich-iannone/SplitR). Andrew Ault (University of Michigan) is acknowledged for discussions of aerosol sampling for INPOP. Funding was provided by US DOE ARM (2016-6841, 2016-6884, and 2016-6875) and Atmospheric Systems Research (ASR) (DE-SC0013306) programs for sample collection/analysis and data interpretation, respectively. Additionally, funding was provided by the NOAA Physical Sciences Division (PSD) to support data and sample analyses. K.A. Pratt and R. Kirpes were supported, in part, by an Early-Career Research Fellowship from the Gulf Research Program of the National Academies of Sciences, Engineering, and Medicine. The content is solely the responsibility of the authors and does not necessarily represent the official views of the Gulf Research Program of the National Academies of Sciences, Engineering, and Medicine. CCSEM-EDX analyses were performed at the Environmental Molecular Sciences Laboratory (EMSL), a national scientific user facility located at the Pacific Northwest National Laboratory (PNNL) and sponsored by the Office of Biological and Environmental Research of the US Department of Energy (DOE). PNNL is operated for DOE by Battelle Memorial Institute under contract no. DE-AC06-76RL0 1830. Travel funds to PNNL were provided by the Michigan Space Grant Consortium

**References**

IMS Daily Northern Hemisphere Snow and Ice Analysis at 1 km, 4 km, and 24 km Resolutions, Version 1, 2008, https://doi.org/10.7265/N52R3PMC.

A language and environment for statistical computing. R Foundation for Statistical Computing, 2017.

Albrecht, B. A.: Aerosols, Cloud Microphysics, and Fractional Cloudiness, Science, 245, 1227-1230, 1989.

Alpert, P. A., Aller, J. Y., and Knopf, D. A.: Ice nucleation from aqueous NaCl droplets with and without marine diatoms, Atmos. Chem. Phys., 11, 5539-5555, 2011.

Alpert, P. A., and Knopf, D. A.: Analysis of isothermal and cooling-rate-dependent immersion freezing by a unifying stochastic ice nucleation model, Atmos Chem Phys, 16, 2083-2107, 2016.

Ault, A. P., Peters, T. M., Sawvel, E. J., Casuccio, G. S., Willis, R. D., Norris, G. A., and Grassian, V. H.: Single-Particle SEM-EDX Analysis of Iron-Containing Coarse Particulate Matter in an Urban Environment: Sources and Distribution of Iron within Cleveland, Ohio, Environ Sci Technol, 46, 4331-4339, 2012.

Bergeron, T.: On the physics of cloud and precipitation, 5th Assembly of the U.G.G.I., Paul Dupont, Paris, 1935.

Bigg, E. K.: The Supercooling of Water, P Phys Soc Lond B, 66, 688-694, 1953.

Bigg, E. K.: Ice forming nuclei in the high Arctic, Tellus B, 48, 1996.

Bigg, E. K., and Leck, C.: Cloud-active particles over the central Arctic Ocean, J Geophys Res-Atmos, 106, 32155-32166, 2001.

Bigg, E. K., and Leck, C.: The composition of fragments of bubbles bursting at the ocean surface, J Geophys Res-Atmos, 113, 2008.

Boose, Y., Sierau, B., Garcia, M. I., Rodriguez, S., Alastuey, A., Linke, C., Schnaiter, M., Kupiszewski, P., Kanji, Z. A., and Lohmann, U.: Ice nucleating particles in the Saharan Air Layer, Atmos. Chem. Phys., 16, 9067-9087, 2016a.

Boose, Y., Welti, A., Atkinson, J., Ramelli, F., Danielczok, A., Bingemer, H. G., Plötze, M., Sierau, B., Kanji, Z. A., and Lohmann, U.: Heterogeneous ice nucleation on dust particles sourced from nine deserts worldwide – Part 1: Immersion freezing, Atmos. Chem. Phys., 16, 15075-15095, 2016b.

Borys, R. D.: Studies of ice nucleation by Arctic aerosol on AGASP-II, J. Atmos. Chem., 9, 1989.

Boucher, O., Randall, D., Artaxo, P., Bretherton, C., Feingold, G., Forster, P., Kerminen, V.-M., Kondo, Y., Liao, H., Lohmann, U., Rasch, P., Satheesh, S. K., Sherwood, S., Stevens, B., and Zhang, X. Y.: Clouds and Aerosols, in: Climate Change 2013: The Physical Science Basis. Contribution of Working Group I to the Fifth Assessment Report of the Intergovernmental Panel on Climate Change, edited by: Stocker, T. F., Qin, D., Plattner, G.-K., Tignor, M., Allen, S. K., Boschung, J., Nauels, A., Xia, Y., Bex, V., and Midgley, P. M., Cambridge University Press, Cambridge, United Kingdom and New York, NY, USA, 571–658, 2013.

Bowers, R. M., Lauber, C. L., Wiedinmyer, C., Hamady, M., Hallar, A. G., Fall, R., Knight, R., and Fierer, N.: Characterization of Airborne Microbial Communities at a High-Elevation Site and Their Potential To Act as Atmospheric Ice Nuclei, Applied and Environmental Microbiology, 75, 5121-5130, 2009.

Burrows, S. M., Hoose, C., Pöschl, U., and Lawrence, M. G.: Ice nuclei in marine air: biogenic particles or dust?, Atmos. Chem. Phys., 13, 245-267, 2013.

Cahill, T. A., Feeney, P. J., and Eldred, R. A.: Size Time Composition Profile of Aerosols Using the Drum Sampler, Nucl Instrum Meth B, 22, 344-348, 1987.

Chen, J., Wu, Z., Augustin-Bauditz, S., Grawe, S., Hartmann, M., Pei, X., Liu, Z., Ji, D., and Wex, H.: Ice-nucleating particle concentrations unaffected by urban air pollution in Beijing, China, Atmos. Chem. Phys., 18, 3523-3539, 2018.

Christner, B. C., Morris, C. E., Foreman, C. M., Cai, R. M., and Sands, D. C.: Ubiquity of biological ice nucleators in snowfall, Science, 319, 1214-1214, 2008.

Cohen, J., Pfeiffer, K., and Francis, J. A.: Warm Arctic episodes linked with increased frequency of extreme winter weather in the United States, Nature Communications, 9, 869, 2018.

Coluzza, I., Creamean, J., Rossi, M., Wex, H., Alpert, P., Bianco, V., Boose, Y., Dellago, C., Felgitsch, L., Fröhlich-Nowoisky, J., Herrmann, H., Jungblut, S., Kanji, Z., Menzl, G., Moffett, B., Moritz, C., Mutzel, A., Pöschl, U., Schauperl, M., Scheel, J., Stopelli, E., Stratmann, F., Grothe, H., and Schmale, D.: Perspectives on the Future of Ice Nucleation Research: Research Needs and Unanswered Questions Identified from Two International Workshops, Atmosphere, 8, 138, 2017.

Conen, F., Morris, C. E., Leifeld, J., Yakutin, M. V., and Alewell, C.: Biological residues define the ice nucleation properties of soil dust, Atmos. Chem. Phys., 11, 9643-9648, 2011.

Conen, F., Stopelli, E., and Zimmermann, L.: Clues that decaying leaves enrich Arctic air with ice nucleating particles, Atmos Environ, 129, 91-94, 2016.

Conen, F., Eckhardt, S., Gundersen, H., and Yttri, K. E.: Rainfall drives atmospheric ice-nucleating particles in the coastal climate of southern Norway, Atmos. Chem. Phys., 17, 11065-11073, 2017.

Cox, C. J., Walden, V. P., and Rowe, P. M.: A comparison of the atmospheric conditions at Eureka, Canada, and Barrow, Alaska (2006–2008), Journal of Geophysical Research: Atmospheres, 117, 2012.

Creamean, J. M., Suski, K. J., Rosenfeld, D., Cazorla, A., DeMott, P. J., Sullivan, R. C., White, A. B., Ralph, F. M., Minnis, P., Comstock, J. M., Tomlinson, J. M., and Prather, K. A.: Dust and Biological Aerosols from the Sahara and Asia Influence Precipitation in the Western U.S., Science, 339, 1572-1578, 2013.

Creamean, J. M., Lee, C., Hill, T. C., Ault, A. P., DeMott, P. J., White, A. B., Ralph, F. M., and Prather, K. A.: Chemical properties of insoluble precipitation residue particles, Journal of Aerosol Science, 76, 13-27, 2014.

Creamean, J. M.: Ice Nucleating Particle Sources at Oliktok Point, 2017a,

Creamean, J. M.: Exploratory Ice Nucleation Measurements at Oliktok Field Campaign Report, U.S. Department of Energy, Office of Science, Office of Biological and Environmental Research, Boulder, CO, 2017b.

Creamean, J. M., Maahn, M., de Boer, G., McComiskey, A., Sedlacek, A. J., and Feng, Y.: The influence of local oil exploration and regional wildfires on summer 2015 aerosol over the North Slope of Alaska, Atmos. Chem. Phys., 18, 555-570, 2018a.

Creamean, J. M., Primm, K. M., Tolbert, M. A., Hall, E. G., Wendell, J., Jordan, A., Sheridan, P. J., Smith, J., and Schnell, R. C.: HOVERCAT: A novel aerial system for evaluation of aerosol-cloud interactions, Atmos. Meas. Tech., submitted, 2018b.

Cziczo, D. J., Ladino, L., Boose, Y., Kanji, Z. A., Kupiszewski, P., Lance, S., Mertes, S., and Wex, H.: Measurements of Ice Nucleating Particles and Ice Residuals, Meteorological Monographs, 58, 8.1-8.13, 2017.

de Boer, G., Eloranta, E. W., and Shupe, M. D.: Arctic Mixed-Phase Stratiform Cloud Properties from Multiple Years of Surface-Based Measurements at Two High-Latitude Locations, Journal of the Atmospheric Sciences, 66, 2874-2887, 2009.

DeMott, P. J., Chen, Y., Kreidenweis, S. M., Rogers, D. C., and Sherman, D. E.: Ice formation by black carbon particles, Geophys Res Lett, 26, 2429-2432, 1999.

DeMott, P. J., Prenni, A. J., Liu, X., Kreidenweis, S. M., Petters, M. D., Twohy, C. H., Richardson, M. S., Eidhammer, T., and Rogers, D. C.: Predicting global atmospheric ice nuclei distributions and their impacts on climate, P Natl Acad Sci USA, 107, 11217-11222, 2010.

DeMott, P. J., Prenni, A. J., McMeeking, G. R., Sullivan, R. C., Petters, M. D., Tobo, Y., Niemand, M., Möhler, O., Snider, J. R., Wang, Z., and Kreidenweis, S. M.: Integrating laboratory and field data to quantify the immersion freezing ice nucleation activity of mineral dust particles, Atmos. Chem. Phys., 15, 393-409, 2015.

DeMott, P. J., Hill, T. C. J., McCluskey, C. S., Prather, K. A., Collins, D. B., Sullivan, R. C., Ruppel, M. J., Mason, R. H., Irish, V. E., Lee, T., Hwang, C. Y., Rhee, T. S., Snider, J. R., McMeeking, G. R., Dhaniyala, S., Lewis, E. R., Wentzell, J. J. B., Abbatt, J., Lee, C., Sultana, C. M., Ault, A. P., Axson, J. L., Diaz Martinez, M., Venero, I., Santos-Figueroa, G., Stokes, M. D., Deane, G. B., Mayol-Bracero, O. L., Grassian, V. H., Bertram, T. H., Bertram, A. K., Moffett, B. F., and Franc, G. D.: Sea spray aerosol as a unique source of ice nucleating particles, Proceedings of the National Academy of Sciences, 113, 5797-5803, 2016.

Despres, V. R., Huffman, J. A., Burrows, S. M., Hoose, C., Safatov, A. S., Buryak, G., Frohlich-Nowoisky, J., Elbert, W., Andreae, M. O., Poschl, U., and Jaenicke, R.: Primary biological aerosol particles in the atmosphere: a review, Tellus B, 64, 2012.

Di Pierro, M., Jaegle, L., Eloranta, E. W., and Sharma, S.: Spatial and seasonal distribution of Arctic aerosols observed by the CALIOP satellite instrument (2006–2012), Atmos. Chem. Phys., 13, 7075-7095, 2013.

Dong, X., Xi, B., Crosby, K., Long, C. N., Stone, R. S., and Shupe, M. D.: A 10 year climatology of Arctic cloud fraction and radiative forcing at Barrow, Alaska, Journal of Geophysical Research: Atmospheres, 115, 2010.

Draxler, R. R.: HYSPLIT4 user's guide, NOAA Air Resources Laboratory, Silver Spring, MD., 1999.

Draxler, R. R., and Rolph, G.: HYSPLIT (HYbrid Single-Particle Lagrangian Integrated Trajectory) Model access via NOAA ARL READY website (http://ready.arl.noaa.gov/hysplit.php), NOAA Air Resources Laboratory, Silver Spring, MD, 2011.

Durant, A. J., Shaw, R. A., Rose, W. I., Mi, Y., and Ernst, G. G. J.: Ice nucleation and overseeding of ice in volcanic clouds, Journal of Geophysical Research: Atmospheres, 113, n/a-n/a, 2008.

Fetterer, F., Stewart, J. S., and Meier, W.: MASAM2: Daily 4 km Arctic Sea Ice Concentration, Version 1., 2015, https://doi.org/10.7265/N5ZS2TFT.

Findeisen, W.: Kolloid-meteorologische Vorgänge bei Neiderschlags-bildung, Meteor. Z., 55, 121-133, 1938.

Fountain, A. G., and Ohtake, T.: Concentrations and Source Areas of Ice Nuclei in the Alaskan Atmosphere, Journal of Climate and Applied Meteorology, 24, 377-382, 1985.

Fridlind, A. M., Diedenhoven, B. v., Ackerman, A. S., Avramov, A., Mrowiec, A., Morrison, H., Zuidema, P., and Shupe, M. D.: A FIRE-ACE/SHEBA Case Study of Mixed-Phase Arctic Boundary Layer Clouds: Entrainment Rate Limitations on Rapid Primary Ice Nucleation Processes, Journal of the Atmospheric Sciences, 69, 365-389, 2012.

Fröhlich-Nowoisky, J., Hill, T. C. J., Pummer, B. G., Yordanova, P., Franc, G. D., and Pöschl, U.: Ice nucleation activity in the widespread soil fungus *Mortierella alpina*, Biogeosciences, 12, 1057-1071, 2015.

Garrett, T. J., and Zhao, C. F.: Increased Arctic cloud longwave emissivity associated with pollution from mid-latitudes, Nature, 440, 787-789, 2006.

Garrett, T. J., Zhao, C. F., and Novelli, P. C.: Assessing the relative contributions of transport efficiency and scavenging to seasonal variability in Arctic aerosol, Tellus B, 62, 190-196, 2010.

Gunsch, M. J., Kirpes, R. M., Kolesar, K. R., Barrett, T. E., China, S., Sheesley, R. J., Laskin, A., Wiedensohler, A., Tuch, T., and Pratt, K. A.: Contributions of transported Prudhoe Bay oil field emissions to the aerosol population in Utqiaġvik, Alaska, Atmos. Chem. Phys., 17, 10879-10892, 2017.

Hader, J. D., Wright, T. P., and Petters, M. D.: Contribution of pollen to atmospheric ice nuclei concentrations, Atmos Chem Phys, 14, 5433-5449, 2014a.

Hader, J. D., Wright, T. P., and Petters, M. D.: Contribution of pollen to atmospheric ice nuclei concentrations, Atmos. Chem. Phys., 14, 5433-5449, 2014b.

Haga, D. I., Burrows, S. M., Iannone, R., Wheeler, M. J., Mason, R. H., Chen, J., Polishchuk, E. A., Pöschl, U., and Bertram, A. K.: Ice nucleation by fungal spores from the classes *Agaricomycetes*, *Ustilaginomycetes*, and *Eurotiomycetes*, and the effect on the atmospheric transport of these spores, Atmos. Chem. Phys., 14, 8611-8630, 2014.

Hill, T. C. J., DeMott, P. J., Tobo, Y., Fröhlich-Nowoisky, J., Moffett, B. F., Franc, G. D., and Kreidenweis, S. M.: Sources of organic ice nucleating particles in soils, Atmos. Chem. Phys., 16, 7195-7211, 2016.

Hoose, C., Kristjansson, J. E., and Burrows, S. M.: How important is biological ice nucleation in clouds on a global scale?, Environ Res Lett, 5, 2010a.

Hoose, C., Kristjánsson, J. E., Chen, J.-P., and Hazra, A.: A Classical-Theory-Based Parameterization of Heterogeneous Ice Nucleation by Mineral Dust, Soot, and Biological Particles in a Global Climate Model, Journal of the Atmospheric Sciences, 67, 2483-2503, 2010b.

Hoose, C., and Möhler, O.: Heterogeneous ice nucleation on atmospheric aerosols: a review of results from laboratory experiments, Atmos. Chem. Phys., 12, 9817-9854, 2012.

Huffman, J. A., Prenni, A. J., deMott, P. J., Pohlker, C., Mason, R. H., Robinson, N. H., Frohlich-Nowoisky, J., Tobo, Y., Despres, V. R., Garcia, E., Gochis, D. J., Harris, E., Muller-Germann, I., Ruzene, C., Schmer, B., Sinha, B., Day, D. A., Andreae, M. O., Jimenez, J. L., Gallagher, M., Kreidenweis, S. M., Bertram, A. K., and Poschl, U.: High concentrations of biological aerosol particles and ice nuclei during and after rain, Atmos. Chem. Phys., 13, 6151-6164, 2013.

5   Irish, V. E., Elizondo, P., Chen, J., Chou, C., Charette, J., Lizotte, M., Ladino, L. A., Wilson, T. W., Gosselin, M., Murray, B. J., Polishchuk, E., Abbatt, J. P. D., Miller, L. A., and Bertram, A. K.: Ice-nucleating particles in Canadian Arctic sea-surface microlayer and bulk seawater, Atmos. Chem. Phys., 17, 10583-10595, 2017.

Jaenicke, R.: Atmospheric aerosols and global climate, Journal of Aerosol Science, 11, 577-588, 1980.

Jefferson, A.: Aerosol Observing System (AOS) Handbook, ARM Climate Research Facility, DOE/SC-ARM/TR-014, 2011.

10  Kanji, Z. A., Ladino, L. A., Wex, H., Boose, Y., Burkert-Kohn, M., Cziczo, D. J., and Krämer, M.: Overview of Ice Nucleating Particles, Meteorological Monographs, 58, 1.1-1.33, 2017.

Kirpes, R. M., Bondy, A. L., Bonanno, D., Moffet, R. C., Wang, B. B., Laskin, A., Ault, A. P., and Pratt, K. A.: Secondary sulfate is internally mixed with sea spray aerosol and organic aerosol in the winter Arctic, Atmos Chem Phys, 18, 3937-3949, 2018.

Knopf, D. A., Alpert, P. A., Wang, B., and Aller, J. Y.: Stimulation of ice nucleation by marine diatoms, Nature Geoscience, 4, 88, 2010.

15  Korolev, A., McFarquhar, G., Field, P. R., Franklin, C., Lawson, P., Wang, Z., Williams, E., Abel, S. J., Axisa, D., Borrmann, S., Crosier, J., Fugal, J., Krämer, M., Lohmann, U., Schlenczek, O., Schnaiter, M., and Wendisch, M.: Mixed-Phase Clouds: Progress and Challenges, Meteorological Monographs, 58, 5.1-5.50, 2017.

Kyrouac, J.: Aerosol Observing System Surface Meteorology (AOSMET) Instrument Handbook, Argonne National Laboratory, Argonne, IL, USA, DOE/SC-ARM-TR-184, 2016.

20  Langham, E. J., and Mason, B. J.: The Heterogeneous and Homogeneous Nucleation of Supercooled Water, Proc R Soc Lon Ser-A, 247, 493-&, 1958.

Laskina, O., Morris, H. S., Grandquist, J. R., Estillore, A. D., Stone, E. A., Grassian, V. H., and Tivanski, A. V.: Substrate-Deposited Sea Spray Aerosol Particles: Influence of Analytical Method, Substrate, and Storage Conditions on Particle Size, Phase, and Morphology, Environ Sci Technol, 49, 13447-13453, 2015.

25  Law, K. S., and Stohl, A.: Arctic Air Pollution: Origins and Impacts, Science, 315, 1537-1540, 2007.

Leck, C., and Bigg, E. K.: Biogenic particles in the surface microlayer and overlaying atmosphere in the central Arctic Ocean during summer, Tellus B, 57, 305-316, 2005.

Lewis, C. W., Baumgardner, R. E., Stevens, R. K., Claxton, L. D., and Lewtas, J.: Contribution of Woodsmoke and Motor-Vehicle Emissions to Ambient Aerosol Mutagenicity, Environ Sci Technol, 22, 968-971, 1988.

30  Lubin, D., and Vogelmann, A. M.: A climatologically significant aerosol longwave indirect effect in the Arctic, Nature, 439, 453-456, 2006.

Maahn, M., de Boer, G., Creamean, J. M., Feingold, G., McFarquhar, G. M., Wu, W., and Mei, F.: The observed influence of local anthropogenic pollution on northern Alaskan cloud properties, Atmos. Chem. Phys., 17, 14709-14726, 2017.

Markus, T., Stroeve, J. C., and Miller, J.: Recent changes in Arctic sea ice melt onset, freezeup, and melt season length, Journal of Geophysical Research: Oceans, 114, 2009.

35  Mason, R. H., Si, M., Chou, C., Irish, V. E., Dickie, R., Elizondo, P., Wong, R., Brintnell, M., Elsasser, M., Lassar, W. M., Pierce, K. M., Leaitch, W. R., MacDonald, A. M., Platt, A., Toom-Sauntry, D., Sarda-Esteve, R., Schiller, C. L., Suski, K. J., Hill, T. C. J., Abbatt, J. P. D., Huffman, J. A., DeMott, P. J., and Bertram, A. K.: Size-resolved measurements of ice-nucleating particles at six locations in North America and one in Europe, Atmos Chem Phys, 16, 1637-1651, 2016.

McCluskey, C. S., DeMott, P. J., Prenni, A. J., Levin, E. J. T., McMeeking, G. R., Sullivan, A. P., Hill, T. C. J., Nakao, S., Carrico, C. M.,
40      and Kreidenweis, S. M.: Characteristics of atmospheric ice nucleating particles associated with biomass burning in the US: Prescribed burns and wildfires, Journal of Geophysical Research: Atmospheres, 119, 10458-10470, 2014.

McCluskey, C. S., Hill, T. C. J., Malfatti, F., Sultana, C. M., Lee, C., Santander, M. V., Beall, C. M., Moore, K. A., Cornwell, G. C., Collins, D. B., Prather, K. A., Jayarathne, T., Stone, E. A., Azam, F., Kreidenweis, S. M., and DeMott, P. J.: A Dynamic Link between Ice Nucleating Particles Released in Nascent Sea Spray Aerosol and Oceanic Biological Activity during Two Mesocosm Experiments,
45      Journal of the Atmospheric Sciences, 74, 151-166, 2017.

Morris, C. E., Georgakopoulos, D. G., and Sands, D. C.: Ice nucleation active bacteria and their potential role in precipitation, J Phys Iv, 121, 87-103, 2004.

Morris, C. E., Conen, F., Huffman, J. A., Phillips, V., Poschl, U., and Sands, D. C.: Bioprecipitation: a feedback cycle linking Earth history, ecosystem dynamics and land use through biological ice nucleators in the atmosphere, Global Change Biol, 20, 341-351, 2014.

50  Morris, C. E., Soubeyrand, S., Bigg, E. K., Creamean, J. M., and Sands, D. C.: Mapping Rainfall Feedback to Reveal the Potential Sensitivity of Precipitation to Biological Aerosols, Bulletin of the American Meteorological Society, 98, 1109-1118, 2017.

Mossop, S. C., and Thorndike, N. S. C.: The Use of Membrane Filters in Measurements of Ice Nucleus Concentration. I. Effect of Sampled Air Volume, Journal of Applied Meteorology, 5, 474-480, 1966.

Murray, B. J., O'Sullivan, D., Atkinson, J. D., and Webb, M. E.: Ice nucleation by particles immersed in supercooled cloud droplets, Chem
55      Soc Rev, 41, 6519-6554, 2012.

O'Sullivan, D., Murray, B. J., Malkin, T. L., Whale, T. F., Umo, N. S., Atkinson, J. D., Price, H. C., Baustian, K. J., Browse, J., and Webb, M. E.: Ice nucleation by fertile soil dusts: relative importance of mineral and biogenic components, Atmos. Chem. Phys., 14, 1853-1867, 2014.

O'Sullivan, D., Murray, B. J., Ross, J. F., Whale, T. F., Price, H. C., Atkinson, J. D., Umo, N. S., and Webb, M. E.: The relevance of nanoscale biological fragments for ice nucleation in clouds, Sci Rep-Uk, 5, 8082, 2015.

Perry, K. D., Cliff, S. S., and Jimenez-Cruz, M. P.: Evidence for hygroscopic mineral dust particles from the Intercontinental Transport and Chemical Transformation Experiment, J Geophys Res-Atmos, 109, 2004.

Petters, M. D., Parsons, M. T., Prenni, A. J., DeMott, P. J., Kreidenweis, S. M., Carrico, C. M., Sullivan, A. P., McMeeking, G. R., Levin, E., Wold, C. E., Collett, J. L., and Moosmüller, H.: Ice nuclei emissions from biomass burning, Journal of Geophysical Research: Atmospheres, 114, n/a-n/a, 2009.

Petters, M. D., and Wright, T. P.: Revisiting ice nucleation from precipitation samples, Geophys Res Lett, 42, 8758-8766, 2015.

Phillips, V. T. J., DeMott, P. J., and Andronache, C.: An Empirical Parameterization of Heterogeneous Ice Nucleation for Multiple Chemical Species of Aerosol, Journal of the Atmospheric Sciences, 65, 2757-2783, 2008.

Phillips, V. T. J., Andronache, C., Christner, B., Morris, C. E., Sands, D. C., Bansemer, A., Lauer, A., McNaughton, C., and Seman, C.: Potential impacts from biological aerosols on ensembles of continental clouds simulated numerically, Biogeosciences, 6, 987-1014, 2009.

Pratt, K. A., DeMott, P. J., French, J. R., Wang, Z., Westphal, D. L., Heymsfield, A. J., Twohy, C. H., Prenni, A. J., and Prather, K. A.: In situ detection of biological particles in cloud ice-crystals, Nature Geoscience, 2, 397-400, 2009.

Quinn, P. K., Shaw, G., Andrews, E., Dutton, E. G., Ruoho-Airola, T., and Gong, S. L.: Arctic haze: current trends and knowledge gaps, Tellus B, 59, 99-114, 2007.

Radke, L. F., Hobbs, P. V., and Pinnons, J. E.: Observations of Cloud Condensation Nuclei, Sodium-Containing Particles, Ice Nuclei and the Light-Scattering Coefficient Near Barrow, Alaska, Journal of Applied Meteorology, 15, 982-995, 1976.

Satheesh, S. K., and Moorthy, K. K.: Radiative effects of natural aerosols: A review, Atmos Environ, 39, 2089-2110, 2005.

Schill, G. P., and Tolbert, M. A.: Heterogeneous Ice Nucleation on Simulated Sea-Spray Aerosol Using Raman Microscopy, J Phys Chem C, 118, 29234-29241, 2014.

Screen, J. A., and Simmonds, I.: The central role of diminishing sea ice in recent Arctic temperature amplification, Nature, 464, 1334, 2010.

Seinfeld, J. H., and Pandis, S. N.: Atmospheric Chemistry and Physics: From Air Pollution to Climate Change, 3rd Ediiion, Wiley, 2016.

Sesartic, A., Lohmann, U., and Storelvmo, T.: Bacteria in the ECHAM5-HAM global climate model, Atmos Chem Phys, 12, 8645-8661, 2012.

Shupe, M. D., Uttal, T., and Matrosov, S. Y.: Arctic Cloud Microphysics Retrievals from Surface-Based Remote Sensors at SHEBA, Journal of Applied Meteorology, 44, 1544-1562, 2005.

Shupe, M. D., Matrosov, S. Y., and Uttal, T.: Arctic Mixed-Phase Cloud Properties Derived from Surface-Based Sensors at SHEBA, Journal of the Atmospheric Sciences, 63, 697-711, 2006.

Shupe, M. D., Walden, V. P., Eloranta, E., Uttal, T., Campbell, J. R., Starkweather, S. M., and Shiobara, M.: Clouds at Arctic Atmospheric Observatories. Part I: Occurrence and Macrophysical Properties, Journal of Applied Meteorology and Climatology, 50, 626-644, 2010.

Shupe, M. D.: Clouds at Arctic Atmospheric Observatories. Part II: Thermodynamic Phase Characteristics, Journal of Applied Meteorology and Climatology, 50, 645-661, 2011.

Sole, V. A., Papillon, E., Cotte, M., Walter, P., and Susini, J.: A multiplatform code for the analysis of energy-dispersive X-ray fluorescence spectra, Spectrochim Acta B, 62, 63-68, 2007.

Stohl, A.: Characteristics of atmospheric transport into the Arctic troposphere, Journal of Geophysical Research: Atmospheres, 111, 2006.

Stone, R. S., Anderson, G. P., Andrews, E., Dutton, E. G., Shettle, E. P., and Berk, A.: Incursions and radiative impact of Asian dust in northern Alaska, Geophys Res Lett, 34, 2007.

Stopelli, E., Conen, F., Zimmermann, L., Alewell, C., and Morris, C. E.: Freezing nucleation apparatus puts new slant on study of biological ice nucleators in precipitation, Atmos Meas Tech, 7, 129-134, 2014.

Stroeve, J. C., Markus, T., Boisvert, L., Miller, J., and Barrett, A.: Changes in Arctic melt season and implications for sea ice loss, Geophys Res Lett, 41, 1216-1225, 2014.

Szyrmer, W., and Zawadzki, I.: Biogenic and anthropogenic sources of ice-forming nuclei: A review, Bulletin of the American Meteorological Society, 78, 209-228, 1997.

Tesson, S. V. M., Skjøth, C. A., Šantl-Temkiv, T., and Löndahl, J.: Airborne Microalgae: Insights, Opportunities and Challenges, Applied and Environmental Microbiology, 2016.

Tobo, Y., DeMott, P. J., Hill, T. C. J., Prenni, A. J., Swoboda-Colberg, N. G., Franc, G. D., and Kreidenweis, S. M.: Organic matter matters for ice nuclei of agricultural soil origin, Atmos. Chem. Phys., 14, 8521-8531, 2014.

Tobo, Y.: An improved approach for measuring immersion freezing in large droplets over a wide temperature range, Sci Rep-Uk, 6, 2016.

Twomey, S.: The Influence of Pollution on the Shortwave Albedo of Clouds, Journal of the Atmospheric Sciences, 34, 1149-1152, 1977.

U.S. Energy Information Administration, I. S. A.: Top 100 U.S. Oil and Gas Fields, Washington, D.C., 2015.

Umo, N. S., Murray, B. J., Baeza-Romero, M. T., Jones, J. M., Lea-Langton, A. R., Malkin, T. L., O'Sullivan, D., Neve, L., Plane, J. M. C., and Williams, A.: Ice nucleation by combustion ash particles at conditions relevant to mixed-phase clouds, Atmos. Chem. Phys., 15, 5195-5210, 2015.

Vali, G.: Sizes of atmospheric ice nuclei, Nature, 212, 384-385, 1966.

5    Vali, G., and Stansbury, E. J.: Time-Dependent Characteristics of Heterogeneous Nucleation of Ice, Can J Phys, 44, 477-+, 1966.

Vali, G.: Quantitative Evaluation of Experimental Results an the Heterogeneous Freezing Nucleation of Supercooled Liquids, Journal of the Atmospheric Sciences, 28, 402-409, 1971.

VanCuren, R. A., Cahill, T., Burkhart, J., Barnes, D., Zhao, Y. J., Perry, K., Cliff, S., and McConnell, J.: Aerosols and their sources at Summit Greenland - First results of continuous size- and time-resolved sampling, Atmos Environ, 52, 82-97, 2012.

10   Vergara-Temprado, J., Murray, B. J., Wilson, T. W., O'Sullivan, D., Browse, J., Pringle, K. J., Ardon-Dryer, K., Bertram, A. K., Burrows, S. M., Ceburnis, D., DeMott, P. J., Mason, R. H., O'Dowd, C. D., Rinaldi, M., and Carslaw, K. S.: Contribution of feldspar and marine organic aerosols to global ice nucleating particle concentrations, Atmos. Chem. Phys., 17, 3637-3658, 2017.

Wegener, A.: Thermodynamik der Atmosphäre, Leipzig, 1911.

Weinbruch, S., Wiesemann, D., Ebert, M., Schutze, K., Kallenborn, R., and Strom, J.: Chemical composition and sources of aerosol particles
15   at Zeppelin Mountain (Ny Alesund, Svalbard): An electron microscopy study, Atmos Environ, 49, 142-150, 2012.

Wilson, T. W., Ladino, L. A., Alpert, P. A., Breckels, M. N., Brooks, I. M., Browse, J., Burrows, S. M., Carslaw, K. S., Huffman, J. A., Judd, C., Kilthau, W. P., Mason, R. H., McFiggans, G., Miller, L. A., Najera, J. J., Polishchuk, E., Rae, S., Schiller, C. L., Si, M., Temprado, J. V., Whale, T. F., Wong, J. P. S., Wurl, O., Yakobi-Hancock, J. D., Abbatt, J. P. D., Aller, J. Y., Bertram, A. K., Knopf, D. A., and Murray, B. J.: A marine biogenic source of atmospheric ice-nucleating particles, Nature, 525, 234-+, 2015.

20   Wright, T. P., and Petters, M. D.: The role of time in heterogeneous freezing nucleation, J Geophys Res-Atmos, 118, 3731-3743, 2013.

**Table 1: Dates and start times of sample collection during INPOP (2017) for samples analysed for INPs. Samples correspond to 1 full day (24 hours from the start time). The "INPs" column corresponds to the stages that were analysed via the DFCP per daily sample. A = 2.96 – >12 µm, B = 1.21 – 2.96 µm, C = 0.34 – 1.21 µm, and D = 0.15 – 0.34 µm.**

| Date | Start (UTC) | INPs |
|---|---|---|
| 11-Mar | 21:00 | A, C |
| 18-Mar | 20:00 | A, C |
| 25-Mar | 20:00 | A, C |
| 01-Apr | 20:00 | A, C |
| 17-Apr | 16:00 | A, B, C, D |
| 24-Apr | 16:00 | A, B, C, D |
| 02-May | 16:00 | A, B, C, D |
| 09-May | 16:00 | A, B, C, D |
| 16-May | 16:30 | A, B, C, D |
| 22-May | 16:30 | A, B, C, D |
| 23-May | 16:30 | A, B, C, D |
| 24-May | 16:30 | A, B, C, D |
| 25-May | 16:30 | A, B, C, D |
| 26-May | 16:30 | A, B, C, D |
| 27-May | 16:30 | A, B, C, D |
| 28-May | 16:30 | A, B, C, D |
| 29-May | 16:30 | A, B, C, D |

**Table 2: Comparison of atmospheric immersion mode INPs measurements presented here with previous studies in the Arctic. Study reference, location, dates, and average INP concentrations converted to $L^{-1}$ reported for up to the four different temperatures shown. The superscripts g, s, and a represent ground-based, shipborne, and airborne measurements, respectively. "None" refers to no reported concentrations (or observed, in the case of the current study) measured at that temperature.**

| Study | Location | Dates | Max volume of air (L) | INPs$_{-10}$ ($L^{-1}$) | INPs$_{-15}$ ($L^{-1}$) | INPs$_{-20}$ ($L^{-1}$) | INPs$_{-25}$ ($L^{-1}$) |
|---|---|---|---|---|---|---|---|
| Bigg (1996) | High Arctic[g] | early Aug 1991 | 3000 | none | $1 \times 10^{-2}$ | none | none |
| | | Aug – Oct 1991 | | none | $3 \times 10^{-3}$ | none | none |
| Borys (1989) | Alaska, Canada, Greenland[a] | Apr 1986 | 1400 | none | $2 \times 10^{-2}$ | none | $5 \times 10^{-1}$ |
| Conen et al. (2016) | Norway[g] | Jul 2015 | 24000 | $6 \times 10^{-4}$ | $7 \times 10^{-3}$ | none | none |
| DeMott et al. (2016) | Bering Sea[s] | Summer 2012 | 13500 | none | $3 \times 10^{-3}$ | $3 \times 10^{-2}$ | none |
| Fountain and Ohtake (1985) | Alaska[g] | Aug 1978 – Apr 1979 | 250 | none | none | $1 \times 10^{-1}$ | none |
| Mason et al. (2016) | Canada[g] | Mar – Jul 2014 | 32400* | none | $5 \times 10^{-2}$ | $2 \times 10^{-1}$ | 1 |
| Radke et al. (1976) | Alaska[a] | Mar 1970 | 3000 | none | none | $2 \times 10^{-2}$ | none |
| This study (2018) | Alaska[g] | Mar – May 2017 | 38428 | $8 \times 10^{-4}$ | $5 \times 10^{-3}$ | $2 \times 10^{-2}$ | $4 \times 10^{-2}$ |
| | | Mar 2017 | | none | $7 \times 10^{-4}$ | $6 \times 10^{-3}$ | $3 \times 10^{-2}$ |
| | | Apr 2017 | | $7 \times 10^{-5}$ | $2 \times 10^{-3}$ | $1 \times 10^{-2}$ | $7 \times 10^{-2}$ |
| | | May 2017 | | $1 \times 10^{-3}$ | $8 \times 10^{-3}$ | $2 \times 10^{-2}$ | $4 \times 10^{-2}$ |
| | | late May 2017 | | $2 \times 10^{-3}$ | $1 \times 10^{-2}$ | $3 \times 10^{-2}$ | $4 \times 10^{-2}$ |

*Not directly provided by citation. Estimated from average total volume of air per sample and standard flow rate specification for the sampler.
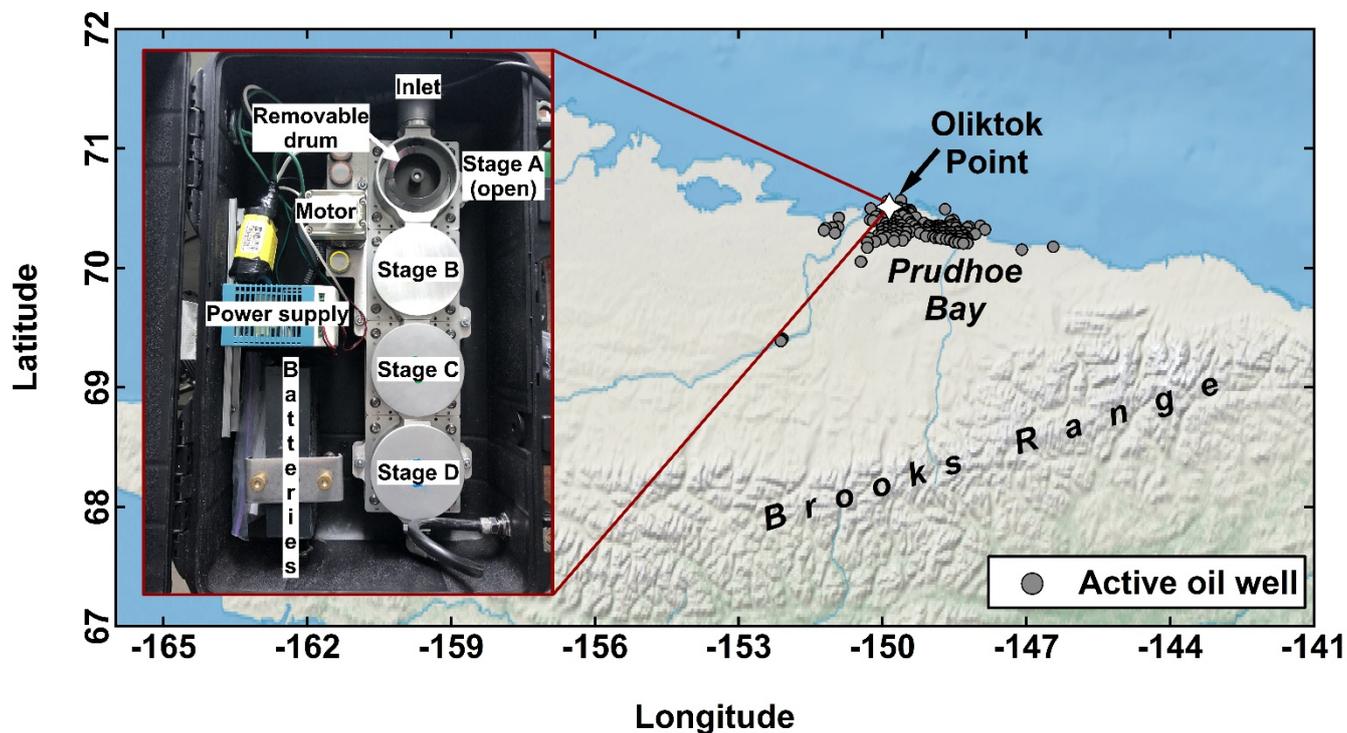
**Figure 1: Map of the North Slope of Alaska highlighting Oliktok Point and oil wells that are active in Prudhoe Bay (data obtained from http://doa.alaska.gov/ogc/publicdb.html in Mar 2017). The approximate areas of Prudhoe Bay and the Brooks Mountain range are shown. Inset shows the inside of the DRUM case, with stage A exposed (i.e., cover removed) and major components labelled.**
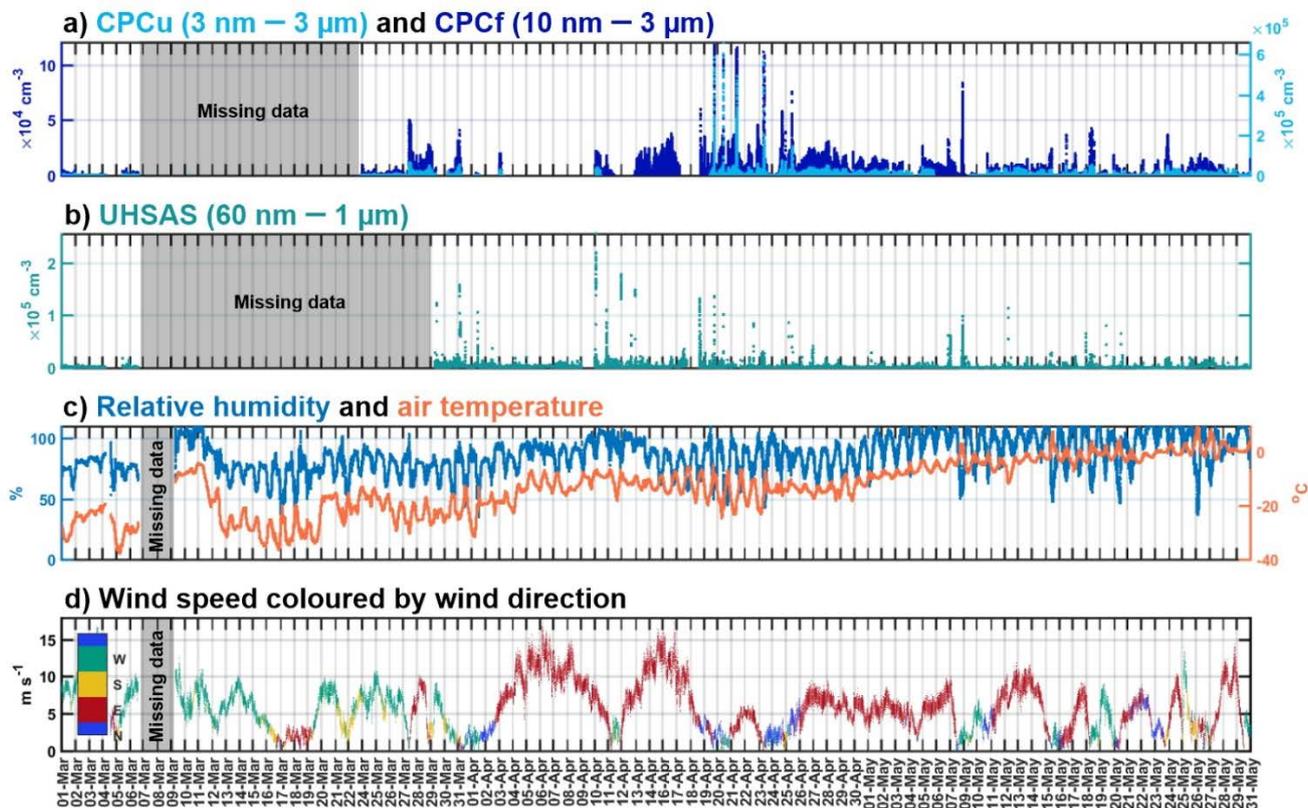
**Figure 2: Time series of 1-second aerosol number and meteorological variables from AOSMET during 1 Mar – 31 May 2017, including aerosol number concentrations measured by a) the condensation particle counter (CPCf) and ultrafine CPC (CPCu) and b) the ultrahigh-sensitivity aerosol sizer (UHSAS). Meteorological data include c) relative humidity and air temperature and d) wind speed coloured by wind direction. Grey shading represents times with missing data.**
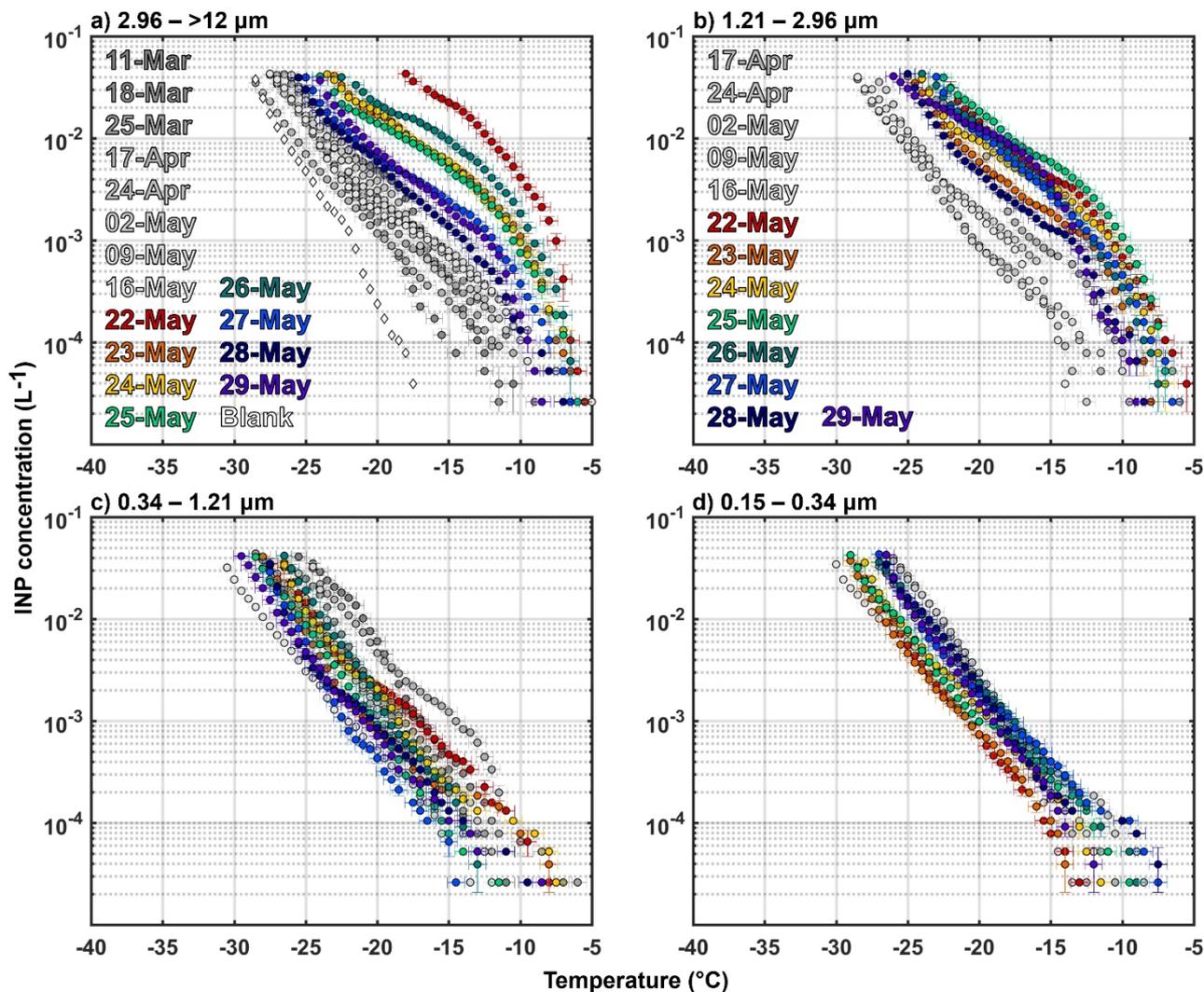
**Figure 3: Cumulative INP spectra for the four size-ranged samples of the DRUM from INPOP. One daily sample per week is shown from 11 Mar to 16 May and 17 Apr to 16 May for stages A/C and B/D, respectively. Daily samples are shown from 22 May – 29 May for all stages. White diamond markers in a) only denote the blank Mylar sample in UPW prepared in the same manner as the samples. This blank spectrum applies to all size ranges.**
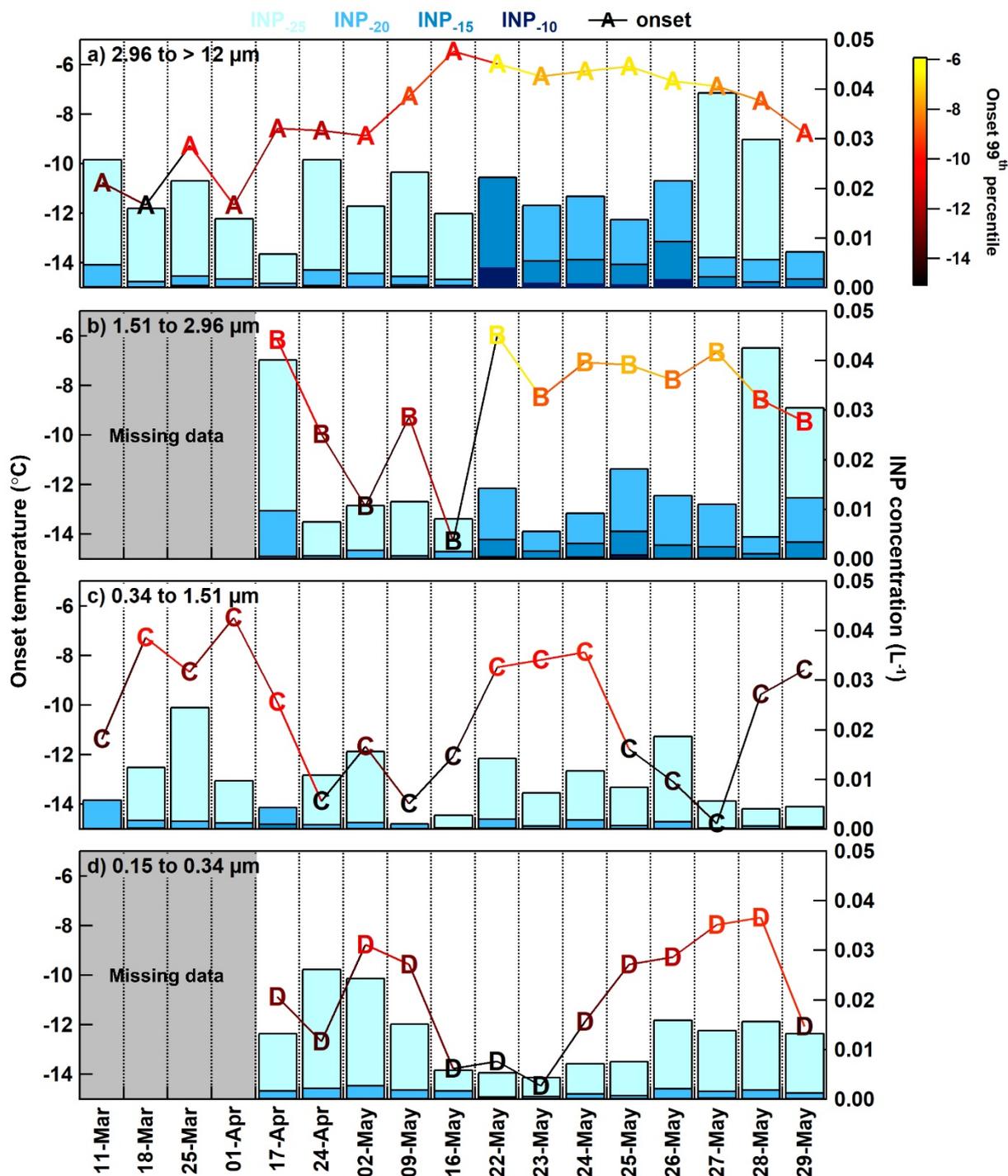
**Figure 4: Onset freezing temperatures and INP concentrations at −10 °C, −15 °C, −20 °C, and −25 °C for DRUM stages a) A, b) B, c) C, and d) D for each sample collected during INPOP. The onset freezing temperatures are coloured by the onset temperature at the 99th percentile. INP-25 concentrations for 22 – 26 May for stages A and B were zero because those all samples froze before −25 °C. Grey shading represents missing data.**
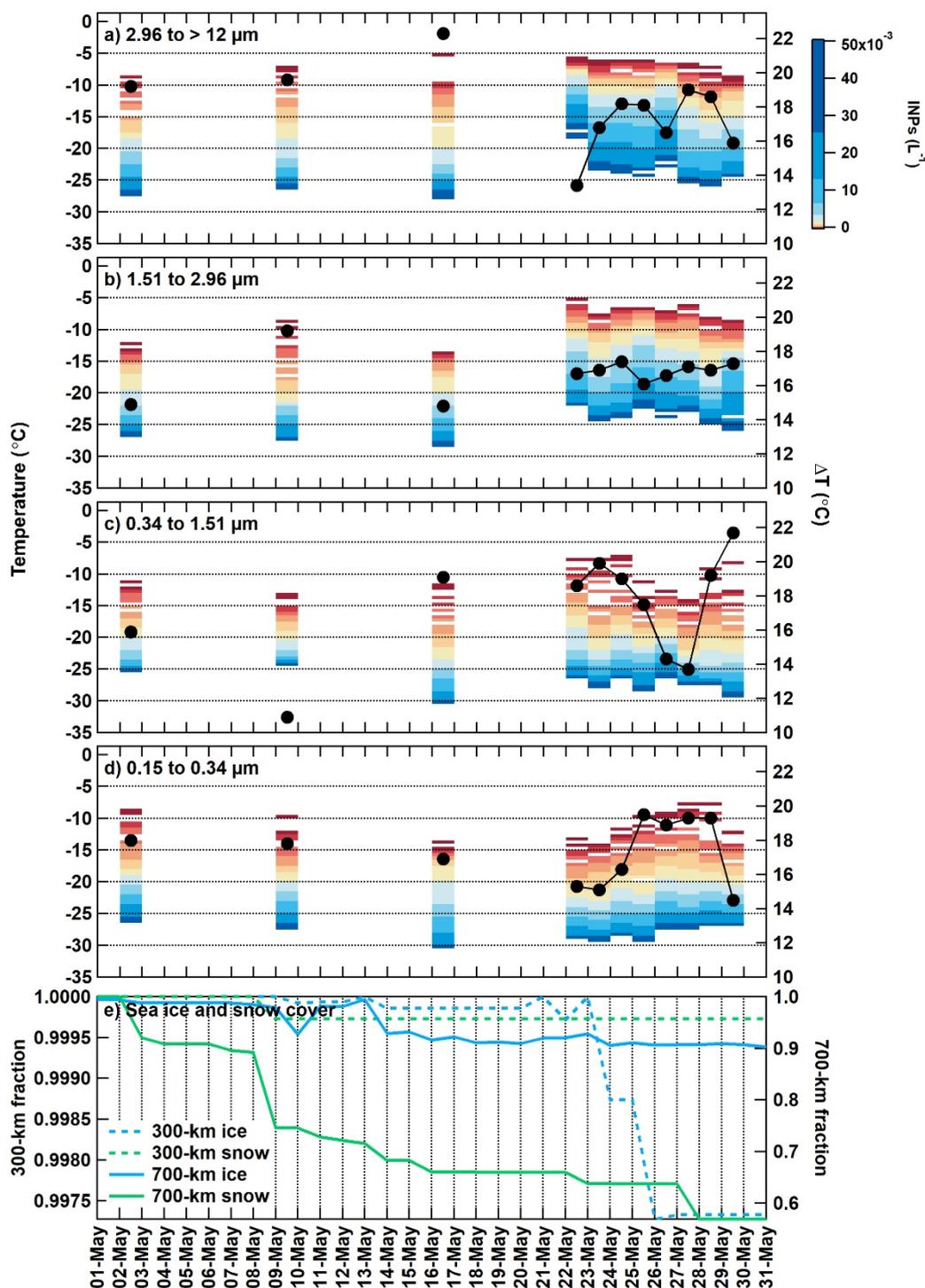
Figure 5: Time series of INP freezing temperatures coloured by INP concentrations (coloured bands, left axis) and ΔT values (black markers, right axis) for DRUM stages a) A, b) B, c) C, and d) D. Also shown are the e) sea ice and snow coverage within a 300-km and 700-km radius from Oliktok Point. Data for the month of May are shown (http://nsidc.org/data/g02156#table3).
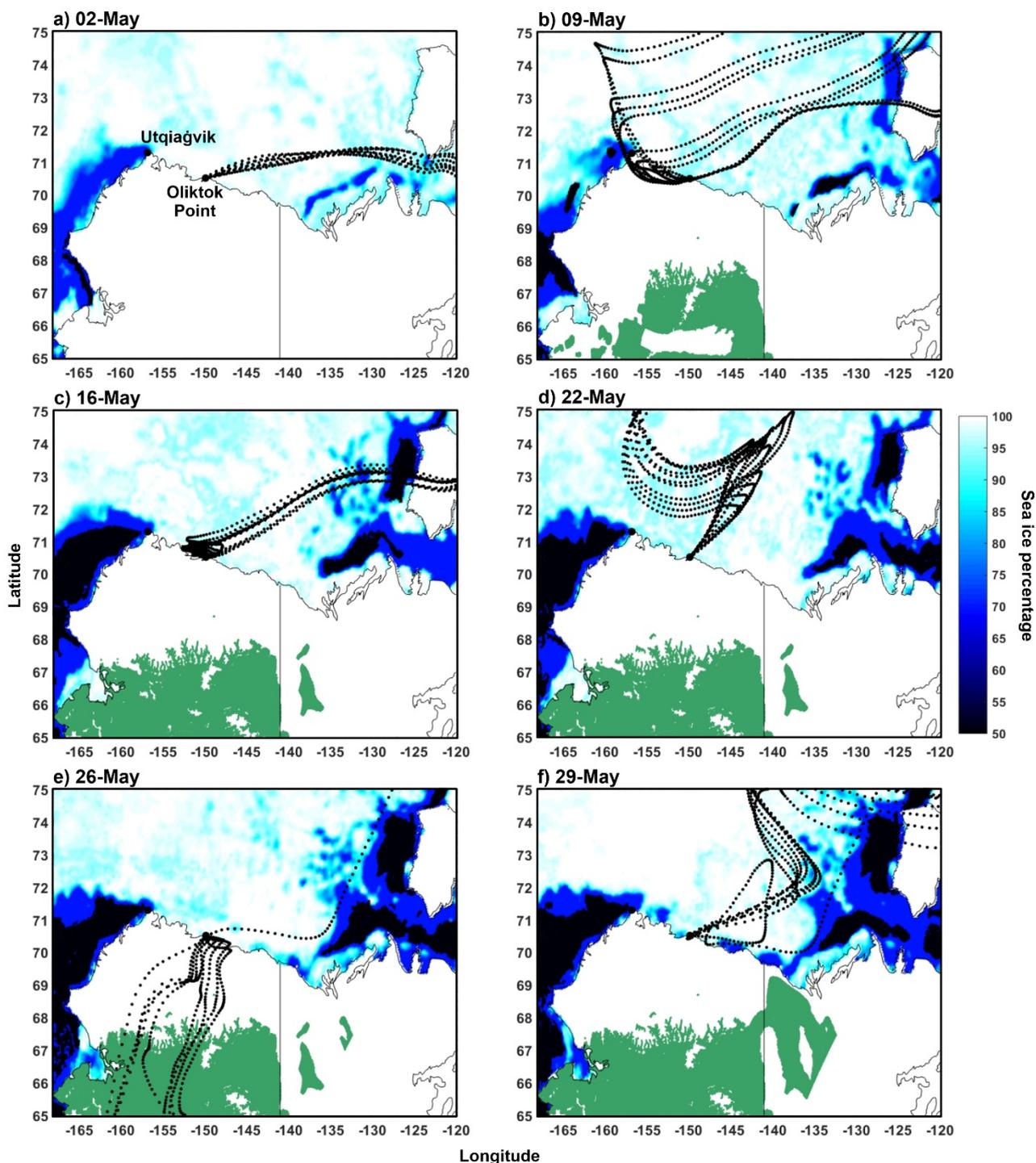
**Figure 6: 5-day air mass backward trajectories initiated every 3 hours and land cover (e.g., sea ice, snow, ocean, and open land) for some of the days in May with INP data. The locations of Utqiaġvik and Oliktok Point are also labelled in panel a) but indicated in all panels by the black circles. On land, white indicates snow covered surfaces while green indicates open land (e.g., tundra).**
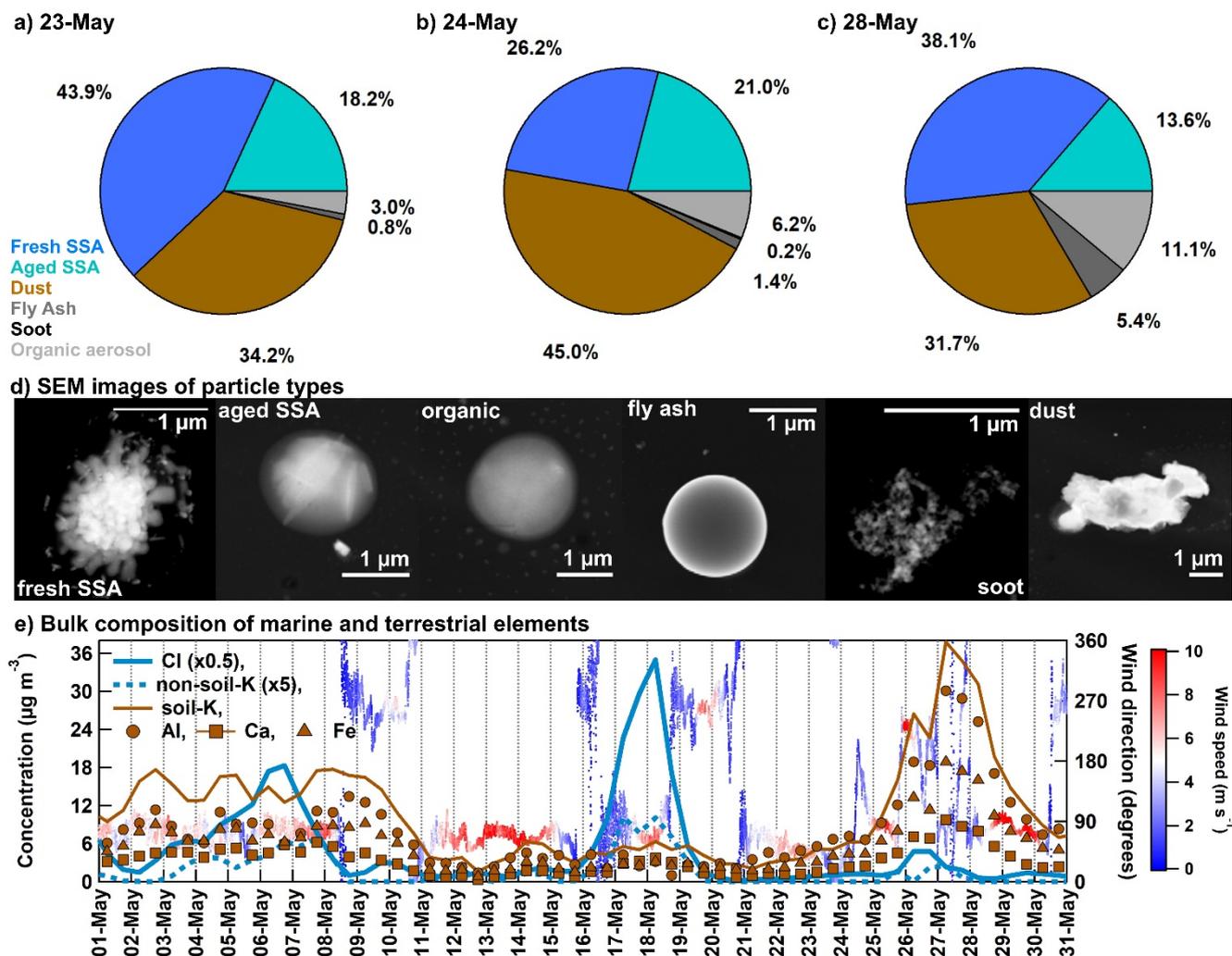
**Figure 7: Summary of results from single-particle and bulk compositional measurements during the late May time period. Relative number fractions of CCSEM-EDX single-particle types for samples (> 1.15 µm) for a) 23 May (1156 particles), a) 24 May (918 particles), and c) 28 May (723 particles). SSA represents sea spray aerosol. Examples of SEM images of the particle types classified are shown in d), with the length of the bar scaled to 1 µm. S-XRF results for May for elements in the 0.75 to 5.0 µm size range associated with either marine (Cl and non-soil-K) or terrestrial (soil-K, Al, Ca, and Fe) sources are shown in e). Cl and non-soil-K concentrations are provided as ×0.5 and ×5 their concentrations, respectively, to show on the same axis. Wind direction is also shown, coloured by wind speed. For both CCSEM-EDX and S-XRF classifications, shades of blue and brown represent marine and terrestrial sources, respectively.**
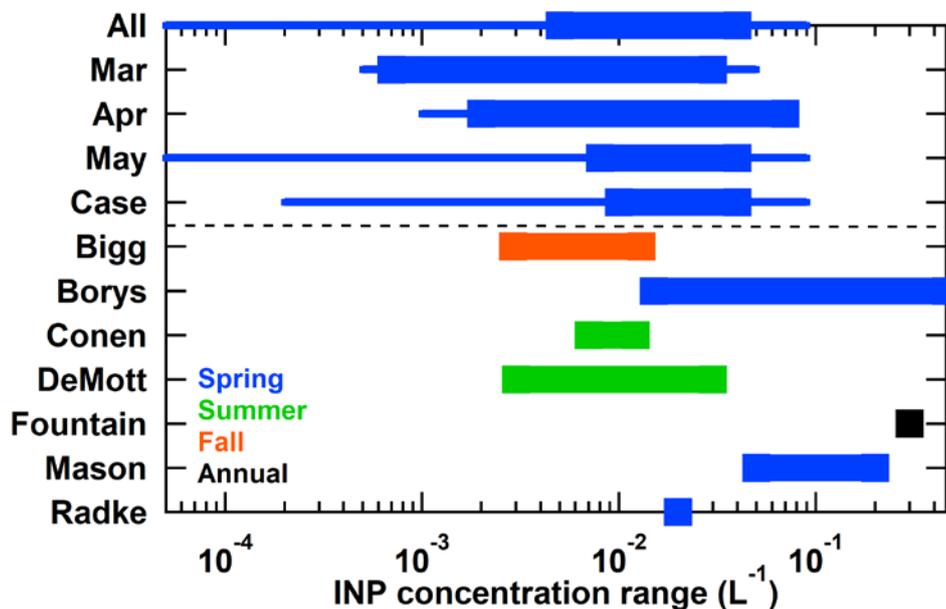
**Figure 8: Summary of ranges of atmospheric immersion mode INP concentrations from the current study and those previously reported in the Arctic. Study details can be found in Table 2. For the current study, "all" and "case" correspond to samples from the entire INPOP study and to the 22 – 29 May time period, respectively. Additionally, the bars and whiskers represent INP concentrations at temperatures in Table 2 and at all temperatures, respectively. Measurements are coloured to the season in which they are predominantly collected during. The dashed line separates results from the current study from those presented in previous works.**